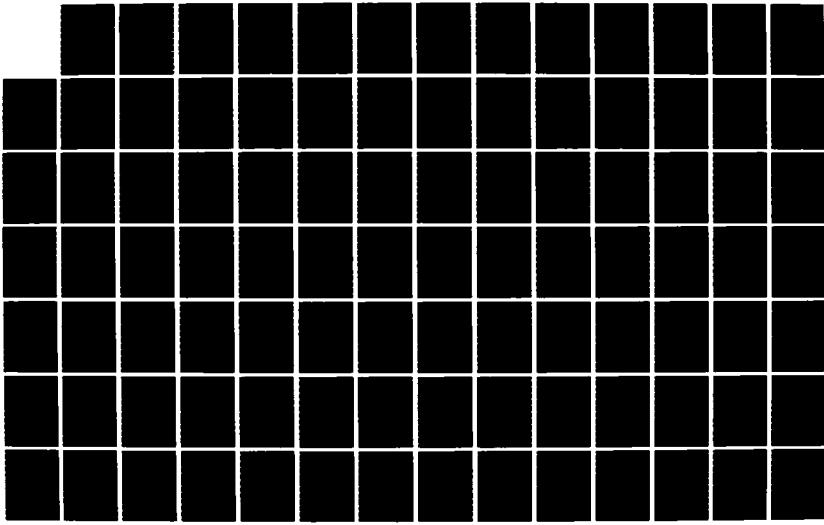


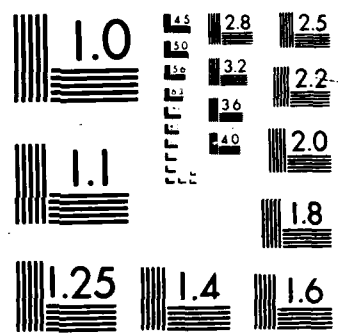
AD-A172 786 A METHOD FOR DETERMINING THE HIGH ENERGY PHOTON 1/2
SPECTRUM OF A PULSED PLASMA SOURCE(U) AIR FORCE INST OF
TECH WRIGHT-PATTERSON AFB OH SCHOOL OF ENGI.

UNCLASSIFIED C W BEASON MAR 84 AFIT/GNE/PH/84M-1

F/G 18/4

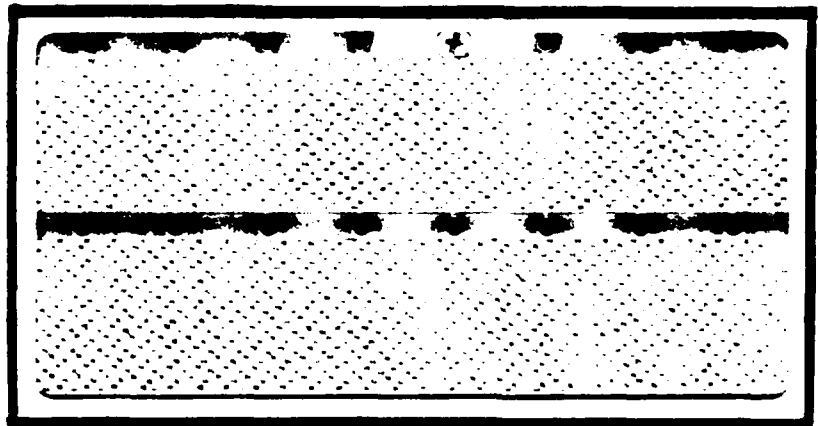
NL





AD-A172 786

DTIC FILE COPY



DISTRIBUTION STATEMENT A
Approved for public release
Distribution Unlimited

DTIC
SELECTED
OCT 1 1986
S B C

DEPARTMENT OF THE AIR FORCE
AIR UNIVERSITY (ATC)
AIR FORCE INSTITUTE OF TECHNOLOGY

Wright-Patterson Air Force Base, Ohio

AFIT/GNE/PH/84M-1

A METHOD FOR DETERMINING
THE HIGH ENERGY PHOTON SPECTRUM OF A
PULSED PLASMA SOURCE
THESIS

Charles W. Beason
Captain, USAF

AFIT/GNE/PH/84M-1

DTIC
SELECTED
OCT 15 1986
S B D

Approved for public release; distributed unlimited.

A METHOD FOR DETERMINING
THE HIGH ENERGY PHOTON SPECTRUM OF A
PULSED PLASMA SOURCE

THESIS

Presented to the Faculty of the School of Engineering
of the Air Force Institute of Technology
Air University
In Partial Fulfullment of the
Requirements for the Degree of
Master of Science in Nuclear Engineering

Charles W. Beason, B.S.

Captain, USAF

March 1984

Approved for public release; distribution unlimited.

Acknowledgments

This thesis is dedicated to the memory of my grandfather,

William Erskine Beason

March 4 1900 - September 29 1983.

I would first like to thank Doctor Bill Baker and the Simulators and Advanced Weapons Concepts Branch at the Air Force Weapons Laboratory (AFWL/NTYP) for providing the financial support for this thesis. I would also like to thank Doctor Jim Degnan of AFWL/NTYP for both the thesis topic and for his guidance and assistance as a Committee Member for the project. I also thank my Committee Chairman, Major John Prince, for his guidance and assistance. Major Larry McKee is also thanked for his assistance as Committee Member.

This project was only a small part of a much larger experimental effort at AFWL/NTYP, and I need to thank those coworkers. They are Second Lieutenant Stephan Warren, Dave Price, Second Lieutenant Mike Snell, and Airman Pete Lagomarsino. I also need to thank Major Jim Lupo of AFWL/NTYP for his efforts in supplying me with copies of computer files.

It is also necessary for me to thank Janet Dahmen and Terri Quinlin for their proof reading skills and moral support.

Finally, I need to thank my family, who have supported me to the fullest throughout this entire effort.

Charles W. Beason

Table of Contents

	Page
Acknowledgments	ii
List of Figures	iv
List of Tables	v
Abstract	vi
I. Introduction	1
II. Theory	6
III. Equipment	26
IV. Procedure	31
V. Results	37
VI. Conclusions and Discussion	52
Appendix A: Listing of Program DCON	54
Appendix B: Sample Input for Program DCON	79
Appendix C: Sample Output for Program DCON	82
Appendix D: Listing of Program PIN	104
Appendix E: Sample Input for Program PIN	113
Bibliography	116
Vita	118

✓

Accession No.	
NTIS No.	
Div.	
Unit	
Date	
By	
Dir.	
Approved	
Dist	
A-1	



List of Figures

Figure	Page
1. Coaxial Plasma Gun	7
2. Plasma Gun Current and Magnetic Field	8
3. SHIVA Z-Pinch Dynamics	10
4. Plasma Gun Z-Pinch Dynamics	12
5. NPM54X Relative Detector Response Normalized To Cobalt 60	38
6. PUFF Plasma Gun Spectrum Shot D6-4, Five Detector Signals Used	43
7. PUFF Plasma Gun Spectrum Shot D6-4, Copper Filtered Detector Signals Varied	44
8. PUFF Plasma Gun Spectrum Shot D6-4, Detector Response Function Varied	47

Abstract

This investigation examined the feasibility of using an array of plastic scintillator photomultiplier tube radiation detectors to determine the high energy ($h\nu > 30$ keV) photon spectrum of SHIVA STAR. A method of determining the spectrum is outlined in which the detectors are filtered with different materials, and the spectrum is deconvoluted by an iterative technique on a computer. Data from SHIVA STAR was not available, so measurements of the radiation output of a plasma gun were analyzed.

List of Tables

Table	Page
I. Detector Filters For PUFF Shot D6-4	41
II. Shot Data For PUFF Shot D6-4	42
III. Parameters For Spectral Power Law Fit	46
IV. List of Experimental Errors	49

I. Introduction

Background

The problem of deconvoluting an unknown spectrum from the responses of differently filtered identical detectors is not a new one. Early work by Ross (14:425; 15:433) involved the use of filters made from two elements of consecutive atomic number. The difference in the energies of the K-edges of the two filtering elements were used to determine the amount of photon energy lying between the K-edges. This technique was later expanded and greatly refined by Kirkpatrick (9:186; 10:223).

The method used by Ross and later by Kirkpatrick allowed the determination of the photon energy in only a narrow region of the electromagnetic spectrum. Silberstein (16:375) reported a method of determining a continuous spectrum, which has been called the Laplace Transform method. However, the drawback in using this method is that the maximum energy of the spectrum needs to be known (19:529).

The present technique used follows that used by Twidell (19:520-539), Tominaga (17:415-421), and exactly that of Degnan (3:264-269). The technique involves performing the deconvolution of the unknown spectrum by an iterative technique on a computer. The deconvolution method used in the computer program is described in the chapter on theory, Chapter II, and is listed in Appendix A.

The spectrum to be determined was to have been the high energy ($h\nu > 20$ keV) photon spectrum of SHIVA STAR. SHIVA STAR

is a large (10 MJ), fast (quarter cycle time of 5 μ sec), capacitor bank used to implode deuterated formvar / aluminum cylindrical liners in a z-pinch at the Simulators and Advanced Weapons Concepts Branch of the Air Force Weapons Laboratory (AFWL/NTYP). Predecessors to SHIVA STAR, such as SHIVA II produced plasmas which radiated several hundred kilojoules of energy in the x-ray region of the spectrum over a period of about 80 nsec. The electron temperature of the plasmas produced were about 300-400 eV in the hottest regions of the pinch (3:267). Fusion of the deuterium in the liners produced on the order of 10^{18} neutrons that were detected by silver activation counters and time-of-flight (TOF) detectors (3:268). The TOF detectors were filtered by 2 in. and 3/8 in. of lead. The difference in signal from the two differently shielded TOF detectors can not be accounted for by assuming that only neutrons are producing the signal. From the signals seen, up to a few joules of high energy photons ($H\nu > 20$ keV) had to have been radiated.

The availability of SHIVA STAR for acquiring experimental data could not be guaranteed, so measurements were taken of the spectrum of the PUFF bank driven coaxial plasma gun at AFWL/NTYP. The PUFF bank is a 500 kJ fast capacitor bank which had a coaxial plasma gun mounted on it. The PUFF bank and the plasma gun are described in the chapter on equipment, Chapter III.

Problem

The problem presented in this thesis is that of devising a method to determine the high energy photon spectrum ($h\nu > 30$ keV) of SHIVA STAR. The method is to be developed using data acquired from a coaxial plasma gun mounted on the PUFF capacitor bank at AFWL/NTYP. The radiation detectors to be used are eight NPM54X plastic scintillator/photomultiplier tube detectors manufactured by EG&G. Filters for the detectors are to be chosen based on estimates of the spectrum. The computer program to be used to deconvolute the spectrum will be a modification of the program XSPEC.

Scope

The scope of this thesis is to be limited to five areas. They are: filter selection, detector calibration, modification of the program XSPEC, spectrum deconvolution, and revised filter selection.

The first area considered is that of filter selection. A reasonable estimate of the expected high energy photon output is first to be made. Filters are then to be chosen based upon what types of filters are available and what combinations of these filters produce a reasonable result from the spectrum deconvolution program.

The detectors are to be calibrated using various radioactive sources that are available. The calibration is to be relative with respect to the photon energies of the sources. An absolute calibration is to be made for each detector from the comparison

of ^{60}Co calibration data provided by the manufacturer of the detectors.

The program XSPEC is to be modified so that it will accept data in the form of time versus detector voltages. The program is to output a spectrum giving photon group energies and energy amounts.

Data from the coaxial plasma gun is to be deconvoluted using the modified program. A spectrum and error estimates will be produced for each set of experimental data deconvoluted.

A revised set of filters based upon the deconvoluted spectrum will be determined.

Assumptions

Several assumptions have to be made concerning this thesis. They are:

- 1) The ^{60}Co calibration data for the NPM54X detectors provided by EG&G is correct to the errors specified;
- 2) The method of deconvolution used by the computer program XSPEC is valid.

Sequence Of Presentation

The sequence of presentation of material in this thesis will be as follows:

- 1) The theories behind the operation of a coaxial plasma gun, the operation of a z-pinch, the radiation detectors, and the method of spectrum deconvolution will be presented in Chapter II;
- 2) The equipment used will be listed and described in Chapter III;

- 3) The procedures followed in detector calibration, filter selection, data acquisition, spectrum deconvolution, and new filter selection will be presented in Chapter IV;
- 4) The experimental results will be presented and described in Chapter V;
- 5) Conclusions and a discussion of the experimental results and their implications will be presented in Chapter VI.

II. Theory

The Plasma Gun

The plasma gun presently used is similar in design and operation to that reported by Marshall (13:134-135). The plasma gun, depicted in Figure 1, is coaxial and is driven by a fast capacitor bank. The capacitor bank drives a high current through a gas that is puffed into the gun at the base of the gun. The current ionizes the puff gas, transforming it into a highly conductive plasma. A magnetic field, \vec{B} , produced by the current, \vec{j} , acts by the $\vec{j} \times \vec{B}$ force to move the current (and thus the plasma) up and out the barrel of the plasma gun at velocities that exceed 10^7 cm/sec (13:134; 1:212).

The $\vec{j} \times \vec{B}$ force acting upon the gas puff can be derived from either Maxwell's equations and the Lorentz force, or by considering the energy density of the self magnetic field as a pressure pushing on the plasma. Figure 2 shows the direction of the current in the plasma, which from the right-hand rule gives the direction of the magnetic field produced by the current in the plasma. Ampere's law gives the conditions requiring the existence of the magnetic field only in the electrode gap beneath the plasma.

As the plasma leaves the gun, two different phenomena could occur. They are the creation of either a focus, a z-pinch, or both. A focus is just a high current discharge, and would be characterized in this configuration by high current arcing through the plasmoid as the plasmoid is leaving the gun.

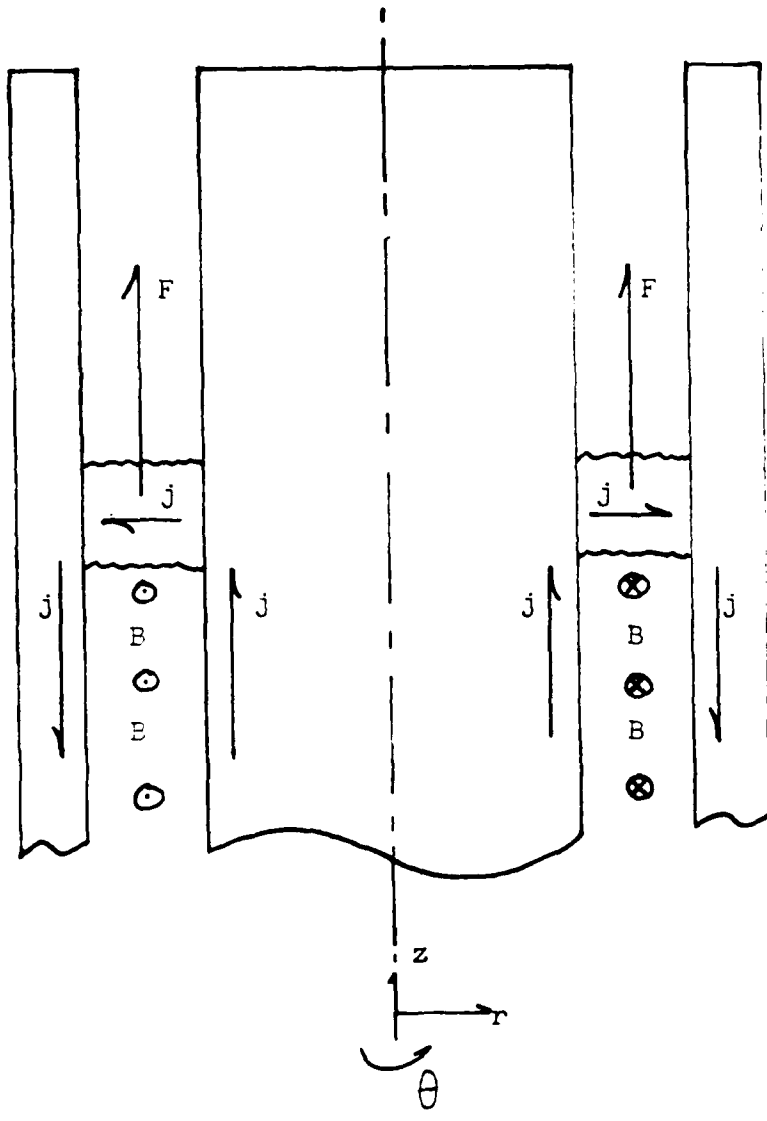


FIGURE 2. Plasma current and tie lines.

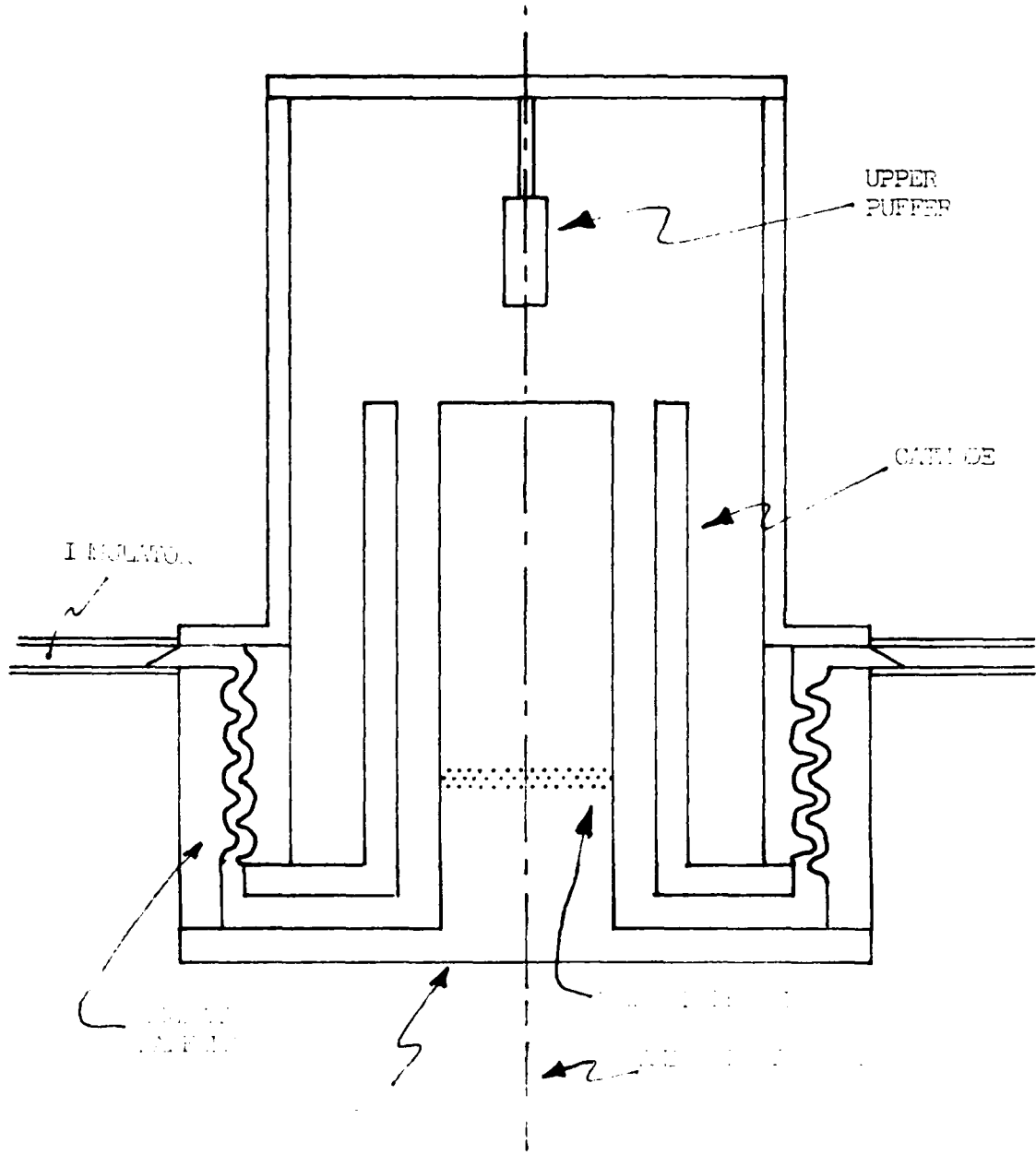


Fig. 1. Multi-Stage Plasma Gun. (Inductor, Capacitor, and Upper Puffer stages shown in cross section)

Any heating of puff gas from a focus would come only from resistive heating, which is self-limiting. A focus is self-limiting because T^4 radiative losses are much higher than the electrical power that can be delivered to a focus. However, this is not true for a z-pinch.

The z-pinch is a electromagnetically driven plasma implosion. Chen (2:304) describes a pinch as follows: 'A plasma carrying a current is confined by the magnetic field of the current itself.' The confining (in this case imploding) force is the $\vec{j} \times \vec{B}$ force (18:4936). The z-pinch is so named because the because the direction of the current that is driving the implosion is along the z-axis. SHIVA (18:4936) and SHIVA STAR experiments are designed to produce z-pinches. In the SHIVA type geometry, as seen in Figure 3, a high current is carried from anode to cathode by a thin cylindrical plasma. The $\vec{j} \times \vec{B}$ force (\vec{j} is in the z direction, \vec{B} in the theta direction) is directed inward (in the negative r direction) towards the z axis. The direction of the magnetic field can be determined from the right-hand rule. The requirement that the magnetic field be zero in the interior of the plasma may be determined from Ampere's law. At the z axis, the plasma collapses on itself where it thermalizes and radiates x-rays as a blackbody. The z-pinch is not self-limiting in the temperature it can reach by electrical power delivery constraints. It is limited only by how much electrical energy can be transformed into kinetic energy of the plasma during the implosion.

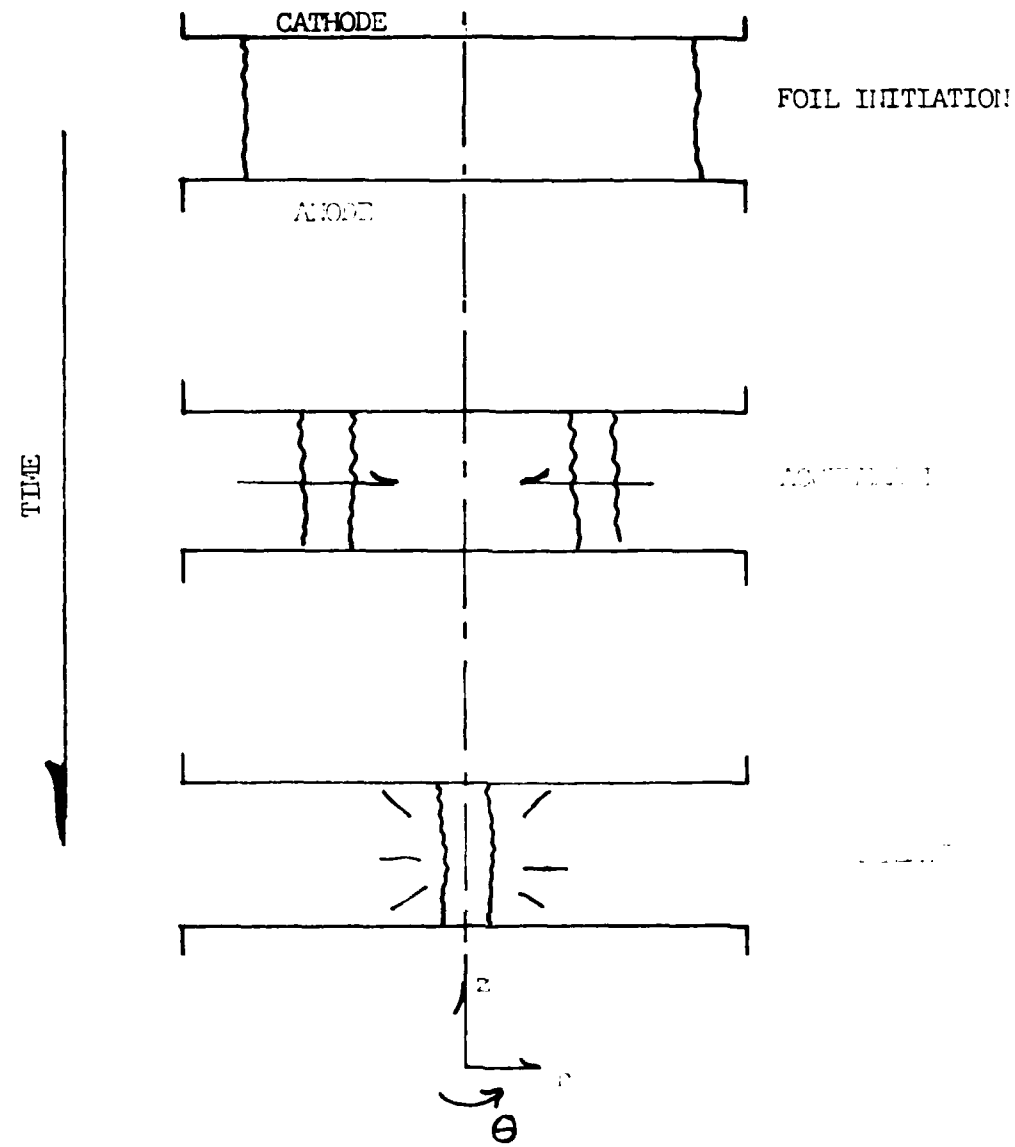
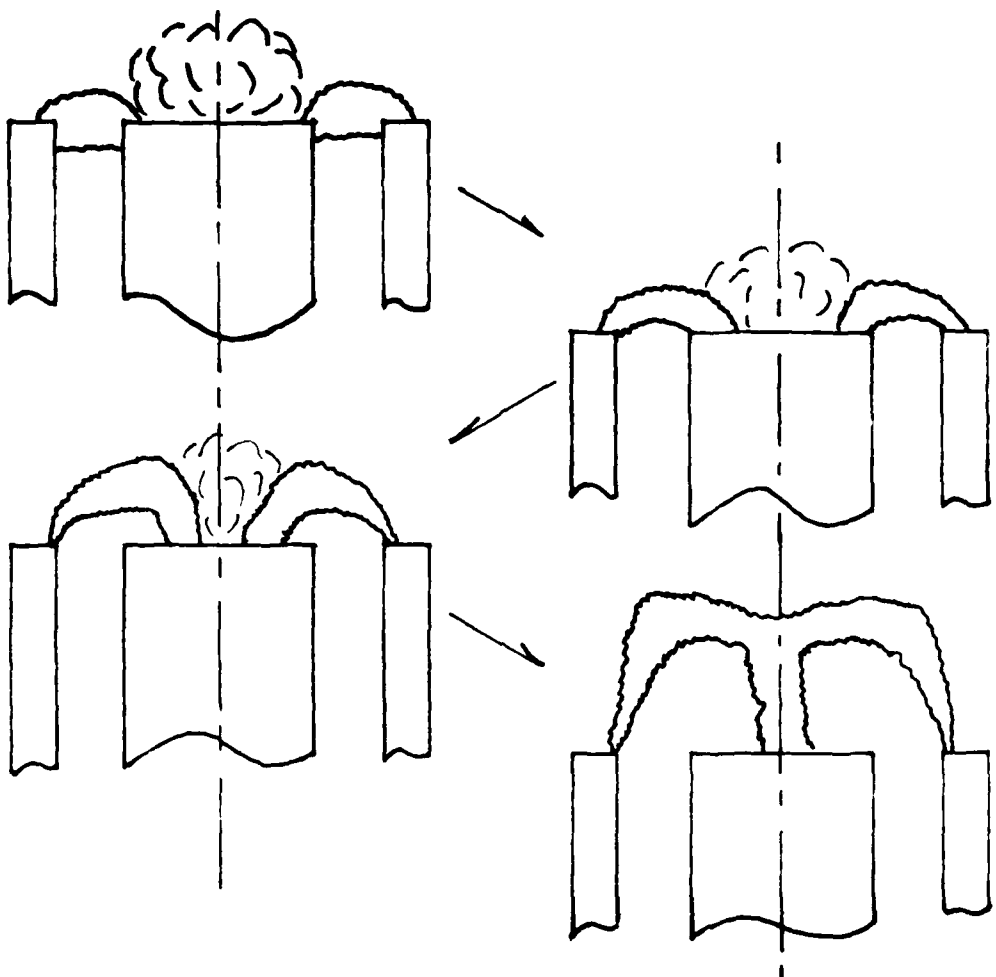


Fig. 1. Foil initiation mechanism.

For the present experiment, a z-pinch would be most likely to occur (if in fact it does) for experiments using the double puff. Figure 4 depicts how a z-pinch would occur in this instance. The plasmoid produced by the plasma gun will act the same as the cathode in the Shiva-type geometry as in Figure 3. The differences in the two geometries are that the cathode will be moving at a very high velocity in the plasma gun driven z-pinch, and that the interior of the liner will be filled with puff gas from the second puffer. The hot plasma produced by a z-pinch would radiate its energy as blackbody radiation.

Blackbody Radiation

A blackbody is a body that absorbs all radiation incident upon it. Also, all blackbodies at the same temperature will emit radiation in the same spectrum (4:5). For a plasma to radiate as a blackbody, a very important condition must be met. Consider the optical path length of a photon of energy equal to the temperature of the plasma. This path length must be short when compared to the size of the plasma. If this condition is met, the plasma will emit radiation similar to that of a blackbody at the same temperature. This forces radiation emitted by the plasma to be in thermal equilibrium with the plasma through many scatters, absorptions, and emissions from when it is initially emitted until it escapes. For the present experiment, it is assumed that if a plasma is produced by either a z-pinch or a focus, the plasma will radiate as a blackbody.



11.1.1. *Lowering the brain.* After the brain is placed in the container, it is lowered slowly. It is important to lower the brain slowly so that the brain does not hit the bottom of the container.

In order to calculate the temperature of any plasma produced by the experiment, it will be first assumed that all of the electrical energy stored in the capacitor bank is coupled into the plasma. The electrical energy stored in the capacitor bank when the bank is charged to $\pm 40\text{ kV}$ is 230 kJ. The power, P , radiated by a blackbody is

$$P = \sigma AT^4 t \quad (1)$$

where T is the temperature of the plasma, A is the surface area of the plasma, and sigma is the Stefan-Boltzmann constant.

Assuming the plasma radiates a constant power for a time t , the energy, E , radiated by the plasma is

$$E = Pt = \sigma AT^4 t \quad (2)$$

The plasma is taken to be a cylinder, where the surface area A is given by

$$A = 2\pi r^2 + 2\pi rh \quad (3)$$

where h is the height and r is the radius of the cylinder.

Solving equation (2) for T , we find

$$T = \sqrt[4]{\frac{E}{\sigma At}} \quad (4)$$

This equation will return the blackbody temperature of the plasma given the energy radiated, the time the energy is radiated, and the surface area through which the energy is radiated.

If the plasma diameter is 0.5 cm, has a length of 2.0 cm, and a radiation time of 100 nsec, the plasma temperature would have to be 50.3 eV in order to radiate 230 kJ. If the diameter was 0.1 cm, the length was 1.0 cm, and the energy was radiated in 10 nsec, the temperature would be 161.8 eV. If the diameter was

0.1 cm, the length was 0.1 cm, and the energy was radiated in 1 nsec, the temperature would be 468.0 eV. It must be remembered that these numbers are extremely unrealistic and err on the high side of any expected blackbody temperature. They are presented in this manner so that blackbody radiation can be ruled out as the production mechanism of the radiation signals seen.

The normalized plankian distribution $P(h\nu)$ is

$$P(h\nu) = \frac{15}{(\pi kT)^4} \frac{(h\nu)^3}{\exp(h\nu/kT) - 1} \quad (5)$$

If kT is taken to be 470 eV and the total energy radiated is 230 kJ, then the plankian distribution numerically integrated from 30 keV to infinity gives $1.84 \times 10^{-18} \exp(-18)$ J as being radiated. The amount of this energy that can pass through the vacuum chamber is given by

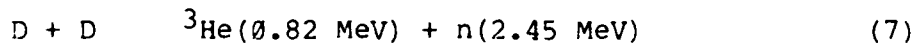
$$E = E_0 \exp(-\sigma\rho x) \quad (6)$$

where sigma is the cross section (for a 30 keV photon passing through iron, sigma is 8.13 cm/gm), rho is the density (for iron rho is 7.874 gm/cm³), x is the thickness of the vacuum chamber (x is 3/8 inch or 0.9525 cm), and E_0 is the integral of equation (5) from kT to infinity times the total energy radiated. Evaluating equation (6) gives the amount of energy between 30 keV and infinity that passes through the vacuum chamber as being 6.02×10^{-45} J or $3.79 \times 10^{-19} \exp(-26)$ eV. There is definitely not enough energy passing through to make up even one 30 keV photon. Integrating (5) for other energies to infinity and evaluating (6) to determine the corresponding attenuation also

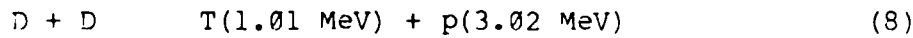
produces similar results. This demonstrates that it is very unlikely that any radiation escaping from the chamber and being detected by the radiation detectors is blackbody radiation.

Fusion Radiation

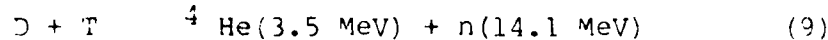
The gas that is puffed into the plasma gun is deuterium. Deuterium, if raised to a high enough temperature, will undergo nuclear fusion through the two nearly equally probable reactions (5 : 15) :



and



The ^3He produced in the first reaction can fuse with deuterium, but the cross section for this reaction is $10 \exp(-4)$ to $10 \exp(-2)$ that of the D-D reaction, so any ^3He -D reactions will be neglected. However, the tritium produced in the second reaction can fuse with deuterium through the reaction (5 :15)



The cross section for this reaction is 50 to 10^3 times that of the D-D reaction, so it would normally be assumed the D-T reaction would occur each time the reaction in equation (8) occurs. This is not the case here, however. The D-T reaction will be assumed to not proceed and will be ignored. This is because if one considers the number of deuterium atoms present (on the order of 10^{18}), compared to a reasonable neutron yield (on the order of 10^9), one finds that a relatively small amount of the deuterium present (four in 10^9)

undergoes fusion. Taking the D-T reaction to be 100 times as likely (four in $10^{exp(7)}$), and 50% of the D-D reactions producing tritium ($2 \times 10^{exp(9)}$), we see that only 50 D-T reactions will occur. Note that this also means that less than one $^3\text{He}-\text{D}$ reaction will occur. The neutrons produced are therefore going to be of one energy, 2.45 MeV.

The neutrons will affect the detectors both directly and indirectly. The direct effect is by the neutrons depositing energy into the scintillating material via proton recoil. The proton will deposit energy by ionization, thus causing a signal. This effect is countered by having one of the detectors filtered with two in. of Pb. The Pb will stop virtually all of the incident photons, but will allow virtually all of the neutrons to pass. The signal from this detector is then subtracted from the signals of the other detectors, thus removing the neutron produced component of their signals.

The indirect method mentioned in the preceding paragraph is fast neutron capture followed by the nearly instantaneous (compared to the plasma radiation pulse length) emission of a gamma ray. This neutron capture radiation is going to be much smaller than the direct neutron induced signals, and will show up as a high energy component in the spectrum if it is large enough to be seen.

Bremsstrahlung Radiation

Bremsstrahlung is radiation produced when a fast charged particle collides with matter and is either stopped or

decelerated. The maximum energy photon produced by bremsstrahlung is equal to the relative kinetic energy between the charged particle and the matter stopping the charged particle.

High voltages (greater than 80 kV) are possible between the electrode and anode in the plasma gun. If electrons are accelerated across this gap without making any collisions with any gas that is left in the plasma gun, the energy of the electrons will be equal to the potential between the electrodes. When these electrons collide with and are stopped by the electrode material (copper), then bremsstrahlung will be emitted. The maximum energy of the bremsstrahlung will thus be equal to the potential between the electrodes.

The maximum voltage between the electrodes can be estimated by knowing dI/dt , which is the change in current with respect to time. This is because the voltage, V , across an inductor (which in the present case is the plasma gun) is given by the equation

$$V = \frac{d}{dt} (IL) = L \frac{dI}{dt} + I \frac{dL}{dt} \quad (10)$$

where L is the inductance of the inductor, I is the total current flowing through the inductor, and t is time. If the circuit had a short in place at the lower puff holes instead of a plasma load, the maximum voltage expected would be 80 kV. This is because the inductance would be constant and maximum dI/dt would occur at time equal to zero, so the voltage is the capacitor charging voltage at that time.

The inductance of the plasma gun is not constant and the load is not a short. The inductance of the load at bank initiation is 20 nH. As the annular plasma reaches the end of the plasma gun, the inductance has risen to 46 nH. As the plasma leaves the plasma gun, the inductance of the circuit rises very quickly. Also, the current drops very rapidly for two reasons. The first is that the current path disappears as the plasma leaves the gun. The second is that the inductance is rapidly increasing.

The dI/dt will be greater than the initial dI/dt . This can be seen by performing a simple calculation. First, the dL/dt term is assumed to be about zero when compared to the dI/dt term because inductance is nearly constant when compared to the change in current expected. Taking 24 in. as the plasma gun length and assuming a constant acceleration time of 3 μ sec (3 μ sec is chosen because as the inductance of the circuit rises, the current rise time in the circuit also rises), the average plasma velocity would have to be $2.0 \times 10^8 \exp(3)$ cm/sec and a final velocity of $4.0 \times 10^8 \exp(8)$ cm/sec (the timing of the bank and the lower puffer are adjusted so that the maximum current occurs as the plasma leaves the gun). If the plasma is 10 cm long, then it would leave the gun and interrupt the current in only 25 nsec. Taking the maximum current of a short for the bank into 46 nH as 3.2 MA, then dI/dt is $1.28 \times 10^{13} \exp(14)$ amps/sec. Multiplying this by 46 nH gives 5.9 MV across the electrodes. This voltage can never be reached, however, because the current will first restrike in the plasma gun. It does make the point though that voltages much higher than the initial 80 kV capacitor bank charge

are possible, and that those voltages are limited by the hold-off voltage of the low density gas that remains behind in the plasma gun after the plasma has left.

It is anticipated that these voltages will be able to accelerate electrons across the electrode gap to voltages as high as 80 keV or even higher. The energy of the electrons will be determined by the density of the gas in the gap which determines the electron path length between collisions. The bremsstrahlung produced will hopefully be observed by radiation detectors that reside outside the vacuum chamber.

Plastic Scintillators and Photomultiplier Tubes

A material that scintillates is a material that exhibits prompt fluorescence when excited electronically (11:240). The radiation detectors used for the present research use plastic for the scintillator material. Atoms in the plastic are electronically excited by the interaction with radiation passing through the plastic. The way the radiation interacts with the plastic depends upon the type of radiation and the energy of the radiation.

Photons can interact with the plastic scintillator in three different ways. They are photoabsorption, Compton scattering, and pair production. In the cases of photoabsorption and pair production, the incident photon completely disappears (11:308).

Pair production occurs when a photon of sufficient energy ($\hbar\nu > 1.022 \text{ MeV}$) interacts via an electromagnetic interaction with a nucleus. The interaction produces an electron-positron pair,

which then proceed to interact further with the plastic scintillator (11:312-313). The positron almost immediately annihilates itself with an electron producing either two 0.511 MeV photons or three photons of varying energies. The dominate method of annihilation produces two 0.511 MeV photons. The two photons then either interact with the plastic via one of the other two interactions, or they escape the plastic. The electron produced can also interact with the plastic. The methods by which it interacts will be considered later in this section.

Compton scattering occurs when a photon scatters off an electron. The energy gained by the electron is equal to the change in energy of the photon (11:309-312). The scattered photon will either again interact with the plastic in one of the three types of interactions mentioned or it will escape. The methods by which the Compton electron interacts will be considered later in this section.

Photoabsorption occurs when a photon interacts with an atom, and the photon completely disappears. In the place of the photon, an energetic photoelectron appears. The energy of the photoelectron is equal to the energy of the incident photon minus the binding energy of the electron to the atom (11:308-309).

The energetic electrons produced by either Compton scattering, photoabsorption, or the electron from pair production interact with the plastic through the electromagnetic interaction. These energetic electrons ionize the plastic and deposit energy as they pass through the plastic. The ionization produces low energy photons that the P-M tube can detect when

recombination of the ions occur. The number and energy of the low energy photons produced in the plastic is proportional to the energy deposited. Thus the low energy photon output of the plastic is proportional to the energy of the fast electrons.

The plastic scintillator presently used is composed completely of carbon and hydrogen. For photon energies of above a hundred keV or so and below 1.5 to 2 MeV, the dominate interaction with carbon and hydrogen is the Compton effect. Therefore, if a pulse height analysis of the output of a photomultiplier tube that is coupled to the plastic scintillator is performed, the pulse height distribution will consist of a Compton edge and a Compton continuum.

A photomultiplier tube consist of two major structures. They are a photocathode section and an electron multiplier section. The photomultiplier tube acts to first use any photon that strikes it to free an electron from the photocathode. The electron is then used to produce a shower of secondary electrons in the electron multiplier section. The number and energy of photons striking the photocathodes is proportional to the energy that has been deposited in the scintillator material. The number of electrons liberated from the photocathode is proportional to the number and energy of photons striking it. The number of secondary electrons produced at all the amplifying stages of the electron multiplier is also proportional to the number of electrons striking them. Therefore, after the final amplifying stage of the photomultiplier tube (at the anode), the charge deposited will be proportional to the energy deposited in the

scintillator material.

The photocathode consists of a material that will emit an electron if a photon strikes it. The probability that a material will undergo photoemission for an incident photon is called its quantum efficiency. This process of photoemission occurs in three stages. First, an incident photon is absorbed with the energy of the photon being transferred to an electron in the photoemissive material. Second, the electron migrates to the surface of the photoemissive material. Third, the electron escapes from the surface of the photocathode.

An electron that escapes from the photocathode is "directed" by the use of electric fields into the electron multiplier section of the photomultiplier tube. The electron is attracted to and strikes a dynode. The dynode will then re-emit several electrons. These electrons are again directed by an electric field to the next dynode, where each electron that strikes it causes the re-emission of several electrons. This continues until after the final dynode is reached, where the anode collects a detectable amount of electrons.

This process works exactly the same way when more than one photon strikes the photocathode. Thus, the current produced by the electrons that are collected on the anode is in direct proportion to the energy deposited in the scintillator material. The energy deposited in the scintillator material is a function of the energy and type of radiation that is incident on the scintillator material. Thus, the current produced by the photomultiplier tube is dependent upon the energy and type of

radiation incident on the scintillator material.

Spectral Deconvolution

As seen in the previous section, the current produced by the type of radiation detectors presently used is proportional to the amount, type, and energy of radiation striking it. It will now be shown that it is possible to use several radiation detectors whose response is like that described above to "back-out" or deconvolute the spectrum of radiation striking them.

In order to do this, first assume we have a radiation source whose spectrum, \underline{x} , consists of discrete energy lines. The strengths of the lines are not known, but their energies are. Also assume the detectors being used have a energy response function, \underline{R} , and the number of detectors used equals the number of energy lines. Third, assume the detectors used to measure this radiation are filtered by filters of different transmission, whose transmission function is \underline{T} . Therefore, the response of the detectors, \underline{b} , will be given by the equation

$$\underline{T} \underline{R} \underline{x} = \underline{b} \quad (11)$$

Taking

$$\underline{A} = \underline{T} \underline{R} \quad (12)$$

we have

$$\underline{A} \underline{x} = \underline{b} \quad (13)$$

The spectrum was assumed to be discrete, so this is just a simple matrix equation where \underline{b} is measured experimentally, \underline{R} is arrived at by calibrating the detectors, and \underline{T} is taken from photon transmission tables. The solution then is found by multiplying

both sides of equation (13) by A^{-1} . This gives

$$\text{or } A^{-1} \underline{A} \underline{x} = A^{-1} \underline{b} \quad (14)$$

$$\underline{x} = A^{-1} \underline{b} \quad (15)$$

The solution thus becomes one of simply finding the inverse of \underline{A} . This is not always trivial, though, as is the case here. The problem is that although \underline{A} is not singular, it is "nearly" singular. A problem like this is called ill-posed, and a matrix like \underline{A} is called "ill-conditioned" (8:2,48). Therefore, many of the usual methods of matrix inversion will not work, so some type of a specialized technique must be used, such as an iterative technique.

An Iterative Technique

Iterative methods are so called "because each method is designed to generate a sequence of vectors (iterates), $\{\underline{x}^{(k)}\}_{k=0}^{\infty}$ which converge to the true solution, \underline{x}_t , of $\underline{A} \underline{x} = \underline{b}$ " (8:60). The iterative technique used here is exactly that used by Degnan et al. (3:264-265). The technique works by solving the following two equations,

$$VC_k(t) = \int R_k(E) S(E) dE \quad (16)$$

and

$$S'(E) = S(E) - \frac{\sum_k R'_k(E) (V_k(t)/VC_k(t))}{\sum_k R'_k(E)} \quad (17)$$

where $V_k(t)$ is the observed signal for the detector k , $VC_k(t)$ is the calculated signal for the detector k , $S(E)$ is the trial spectrum for the present iteration, $S'(E)$ is the corrected

spectrum, $R'_k(E) = R_k(E)/ \int R_k(E) dE$, E is the photon energy, and gamma is 1.2. Gamma is an overcorrection parameter that is used to speed convergence. Equation (17) is called the corrector equation because it modifies or corrects a guess at the spectrum to produce a new guess at the spectrum.

The equations are solved by first calculating several functions that do not change throughout the iterative process. They are $R_k(E)$ which is the response of the kth detector as a function of energy, $R'_k(E)$ which is the normalized response of the kth detector as a function of energy, and $\sum_k R'_k(E)$ which is the sum over the k detectors of $R'_k(E)$. The iterative process consists of taking a guess at the spectrum, $S(E)$, and computing a calculated detector response, VC_k , for that spectrum by integrating equation (16). The calculated detector response is then used in the corrector equation to produce a new guess at the spectrum. This process is repeated until the desired convergence is reached.

The program DCIN that solves equations (16) and (17), is the same program used by Degnan et. al. (3:264-269), except for some restructuring, changes in the input/output routines, and detector response function/filter calculation routine changes. The program is listed in Appendix A, is written in FORTRAN, and as listed will execute on a VAX 11/780 using the UNIX operating system. The program will execute under the VAX/VMS operating system by just modifying the two OPEN statements in subroutine DATIN.

III. Equipment

PUFF Capacitor Bank

The experimental measurements were taken on a large fast capacitor bank called PUFF which is located at the Simulators and Advanced Weapons concepts Branch of the Air Force Weapons Laboratory (AFWL/NTYP) at Kirtland Air Force Base, New Mexico. The PUFF bank consists of 48 six μF capacitors which are operated in a configuration of two groups of 24 capacitors each. The capacitors in each group are connected in parallel, with the two groups connected in series. The capacitance of the bank is 72 μF in this configuration. The bank is charged so that both groups of capacitors are charged to voltages that are opposite in sign, but equal in magnitude. For the present series of experiments, PUFF was charged to either ± 30 , 35, or 40 kV. Charging PUFF to these voltages produces stored electrical energies in the bank of either 129.6, 176.4, or 230.4 kJ, respectively. The inductance of the bank, transmission lines, radiation baffles, and plasma gun up to the gas puff holes in the anode is 20 nH, so the quarter cycle rise time of the bank for a short at that point is 1.9 μsec .

Radiation Baffles

The current from the bank is carried from the vacuum-insulator interface to the load region of the apparatus by a large "screw" or helix (see Figure 1, page 7). The helix acts as a set of radiation baffles, and prevents radiation produced by the plasma from reaching the insulator at the vacuum-insulator

interface. The baffles are necessary because the untra-violet and soft x-ray radiation from the plasma is able to remove electrons from the insulator by the photoelectric effect. If enough electrons are removed from the insulator, electrical breakdown occurs at the vacuum-insulator interface. Electrical breakdown would divert current from the load region. The diversion of current from the load region would degrade the performance of the plasma gun.

Coaxial Plasma Gun

The load region of the apparatus consists of a 24 in. long coaxial plasma gun. The inner diameter of the plasma gun (the anode) is 5 in., and the outer diameter (the cathode) is 7 in. The anode is a hollow copper tube that has 96 1/4 in. holes spaced around the base 13 in. from the top. These holes allow deuterium gas to be puffed into the plasma gun just prior to bank initiation. The gas is puffed into the gun through the holes by the lower puffer. The cathode consists of 24 1/2 in. diameter copper rods equally spaced around the anode, with a one in. gap between the anode and the cathode. The rods that make up the cathode stop even with the top of the anode. The anode is covered with a circular copper plate. There is a second gas puffer located six cm above the center of the copper plate.

The plasma gun operates as follows. First, gas is puffed into the plasma gun by the lower puffer at the base of the gun. The bank is then initiated. As the voltage in the plasma gun increases, the gas breaks down electrically and current, j ,

begins to flow through the gas. The gas is heated resistively, which turns the gas into a plasma. The rising current creates a rising magnetic field, B , beneath the plasma. The $j \times B$ force accelerates the annular plasma upward. The plasma is accelerated up the plasma gun to the end of the plasma gun where it either pinches on itself in a z-pinch, drives a second puff of gas from the upper puffer into a z-pinch, or just departs as what is known as a plasmoid and impacts the plate at the top of the vacuum chamber.

Gas Puffers

The gas that is puffed into the plasma gun is deuterium. Three cubic cm of deuterium at 900 psi is puffed near the base and is directed radially outward in an annulus. The mass of the gas in the coaxial gap is about 1×10^{-3} gm at the time the main capacitor bank discharge is triggered.

A second puff of deuterium comes from a puffer of six cubic cm in volume at 30 psi. This puffer has a single puff hole in it, is aligned along the vertical axis of the anode, and is pointed down at the top of the anode. The mass of deuterium in the second puffer is about 2.7×10^{-4} gm. The second puff occurs six cm above the end of the plasma gun. The timing of the second puff is such that the maximum coupling of energy occurs between the first puff and the bank into the deuterium of the second puff. The amount of energy coupled can be measured by examining either the x-ray output of the pinch, the fusion neutron yield of the pinch, or the voltages and currents of the

experimental apparatus at various locations.

The two puffers are activated by the discharge of small capacitor banks. The first puffer operates by a piston being released. The piston is held in place by a small (one in. long by 1/2 in. in diameter) wooden rod. The wooden rod has a 0.005 in. hole along the axis. The hole contains a 0.001 in. diameter copper wire and water. The wire is attached to one of the small capacitor banks. When the capacitor bank fires, the copper wire explodes. The exploding wire heats the water and turns it into steam. The pressure from the steam destroys the wooden rod. The piston is thus released, allowing deuterium to puff into the plasma gun through the puff holes in the anode.

The second puffer is operated by having an electromagnetically driven hammer strike against a re-usable diaphragm. The puffers are similar in design to those used at Sandia National Laboratory and Lawrence Livermore National Laboratory (12:65).

The Detectors

The detectors presently used are called NPM54X, and are built by EG&G. They are sealed integral units consisting of a 2 and 1/4 in. diameter by 2 and 1/4 in. long plastic NE111 cylindrical scintillator coupled to a ND2020 photomultiplier tube. The NE111 is painted black, except for the end coupled to the photomultiplier tube. The scintillator and the photomultiplier tube are encased in a 3/16 in. aluminum jacket, except for the front end, which is only covered by a three mil aluminum foil. Also, the detectors are wrapped in 5/8 inch of lead which

cuts down the amount of scattered radiation incident on the detectors.

The operating voltage of the detectors is -2800 V. They were originally acquired as neutron time-of-flight detectors, and have been used as such for SHIVA I, SHIVA I', SHIVA II, and SHIVA STAR experiments at AFWL/NTYP.

IV. Procedure

Detector Calibration

Calibrating the detectors consists of three steps. The first consists of acquiring pulse height distributions for various energy radioactive sources. The second is to determine relative response functions for the various energies. Step three entails using the ^{60}Co calibration data provided by the manufacturer to produce an absolute calibration.

The first step consists of using a single detector that is connected to a pulse height analysis system to obtain pulse height distributions of a set of calibrated radiation sources. This is done by connecting the output of one of the detectors to a linear amplifier which is connected to a multichannel analyzer (MCA). A calibration source is then placed a known distance from the detector, and the MCA is started. Pulse height data from the detector is taken until a sufficient number of pulses have been recorded. This is repeated for several other calibrated sources of different energies. A background pulse height data run is also performed.

In addition to the pulse height data taken, there is also a need to know what pulse voltage corresponds to what channel in the MCA. This is found by connecting a pulse generator into the linear amplifier where the detector was. Voltage pulses of known voltage are then sent to the MCA, and the corresponding channel number is recorded.

The second step involves taking the data acquired in the

first step and analyzing it on a computer. First, all of the pulse height distributions $n(c)$ are normalized to the same count time of one second.

$$N(c) = n(c)/t \quad (18)$$

where $N(c)$ is the time normalized pulse height distribution, c is the channel number, and t is the count time for $n(c)$ in seconds. The time normalized background pulse height distribution $B(c)$ is then subtracted from the pulse height distributions of the various sources.

$$M(c) = N(c) - B(c) \quad (19)$$

Next, the calibration data of the pulse height analysis system is used to determine what height voltage pulse corresponds to what channel for each channel. These voltages are then multiplied by the number of pulses in each corresponding channel, and the voltage-pulse number products are all summed.

$$S = \sum_c M(c) * V(c) \quad (20)$$

where $V(c)$ are the voltages of the pulses corresponding to each channel c , and S is the sum of all of these voltage-pulse number products. Using the source to detector distance, an area is determined for a sphere of radius equal to that distance. This surface area is divided into the area of the detector presented to the source. This is multiplied by the present activity of the source in counts per second.

$$D = A\pi r^2 / 4\pi R^2 = Ar^2 / 4R^2 \quad (21)$$

where r is the radius of the detector face, R is the source to detector distance, A is the present source activity, and D is the activity passing through the detector. Now, dividing S by D , we

arrive at an average voltage pulse height per count, P.

$$P = S/D \quad (22)$$

If E is the photon energy of radiation in MeV, and that is divided into P, then we obtain the average pulse height per MeV H, for the energy E.

$$H(E) = P/E \quad (23)$$

The above procedure is repeated for several different energy photon sources, so that the function H(E) is determined for several different photon energies. One of the photon sources used must be ^{60}Co so that an absolute calibration may be performed.

The final step is to calibrate each detector separately to its own absolute ^{60}Co calibration data. The absolute calibration is obtained from data provided by the manufacturer of the detectors. The value of H(E) for ^{60}Co is divided into the calibration sensitivity value which has units of Amps-cm²-sec/ γ -MeV. This ratio is then multiplied by the other values of H(E) to obtain the calibration for the other energies obtained when the relative calibration was performed.

Choosing The Filters

The filters for the detectors are chosen by two simple criteria. The first is determining exactly what filters are available. The second is to use the known cross sections of these filters and a resonable predicted spectrum with varying combinations of the filters to calculate detector voltage signals. These detector signals are then used as input to the

program DCON. The set of filters that produces the "best" (i.e. the calculated spectrum is closer to the "original" predicted spectrum, and the error estimated by the program is smaller) results should be used. It should also become apparent that as the original spectrum is changed, the sets of filters that work best also changes.

Acquisition Of Data

The details of data acquisition presented here will only concern the operation of the NPM54X detectors and the method of obtaining current traces for them. The operational procedures of the PUFF bank and its associated equipment will not be presented. There are two reasons for this. The main reason is that the data being acquired by the author was only an ancillary part of a larger effort. The second reason is preparing the bank for a shot and firing the bank requires at least four people performing different tasks simultaneously. Therefore, the author did not perform all of the tasks.

The detector voltage traces were obtained as follows. First, the detectors were placed on a stand such that the centers of all the detectors were in a horizontal plane with an elevation one in. above the anode surface. Then, the filters were mounted on the detectors. Next, the detectors were aligned so that they were pointing at a spot one in. above the center of the anode. After power and signal cables were connected, detector to center of anode measurements were obtained. Power was then applied to the detectors. The oscilloscopes on which the data was taken

were located in a screen room, and personnel in the screen room readied the oscilloscopes for bank firing. The bank was then charged and fired. The voltage traces from the oscilloscopes was recorded on Polaroid film. From knowing the oscilliscope settings and the graticule images on the traces, voltages can be read directly off the traces.

Normally, timing marks or fiducials are added to the voltage traces. It was not possible to add them for this series of experiments because of a serious noise problem the fiducial generator was causing on the traces. For the data presented in the results chapter, pulse timing information is obtained by assuming the voltage peaks in all the traces occurred simultaneously. Also, prior to a shot, fiducials were used to synchronize the traces.

Deconvolution Of Spectrum

The voltages obtained in the manner described in the previous section are entered into a data file that is used as input into a program that acts as a pre-processor to the program DCON. The pre-processor program is called PIN, and it removes any $1/R^2$ dependance the data has and changes the voltages to the appropriate units. PIN then outputs a file that is used as the input file for DCON. The program DCON is then run, and the program outputs a spectrum for the experiment. PIN is listed in Appendix D, and sample input for PIN is listed in Appendix E. Appendix B, the sample input for DCON, is also an example of output from program PIN.

Choosing New Filters

The final step in this process is to choose a new set of radiation filters. This is done by using the spectrum obtained from the spectrum deconvolution step as a predicted spectrum for the program DCON. A program is executed that accepts the spectrum and a set of filters as input. The program outputs detector responses in a format DCON can read. DCON is executed, and it calculates a spectrum. This spectrum is then compared to the experimental spectrum. When the filters used for the experiment are used as input to the program that generates the detector responses, the differences in spectra should give some idea about the error in the experimental spectra that result from non-optimum filter selection. Again, after many different sets of filters are tried, it should become apparent that certain sets of filters work better than others for the actual spectra the plasma gun produces. One of the sets that work best should be used as filters for the next experiment.

V. Results

Detector Calibration

Detector S/N 080-LV was used to perform the relative photon energy calibration. The relative detector response as a function of incident photon energy is shown in Figure 5. The "x's" in the figure is experimental data that has been normalized to a linear least squares fit to the same energy as the ^{60}Co response data. The "dashed" line is the linear regression fit to the data. For the linear regression, the x intercept was calculated to be 0.816 ± 0.151 , and the slope was calculated to be 0.147 ± 0.186 per MeV. The curved "solid" line in Figure 5 shows mass energy absorption coefficients for polystyrene (C_8H_8) (7:74), which is close in chemical composition to NE111 (NE111 is composed entirely of hydrogen and carbon, and has an H:C atom ratio of 1.096:1) (11:246). The data for polystyrene has been log-log interpolated, and as shown is normalized so that the mass energy absorption coefficient at the ^{60}Co photon energy is equal to one. The "dotted" line in the figure is the flat detector response function. The program DCON is written so that any of three relative detector response functions may be used. They are the linear regression, the flat response, or the log-log interpolated polystyrene mass absorption coefficients.

The absolute detector responses are computed in the program DCON by multiplying the relative detector response for the photon energy in question by the response for ^{60}Co that was provided by the manufacturer. It will be shown later that the relative

NPM54X Relative Detector Responses Normalized To Cobalt 60

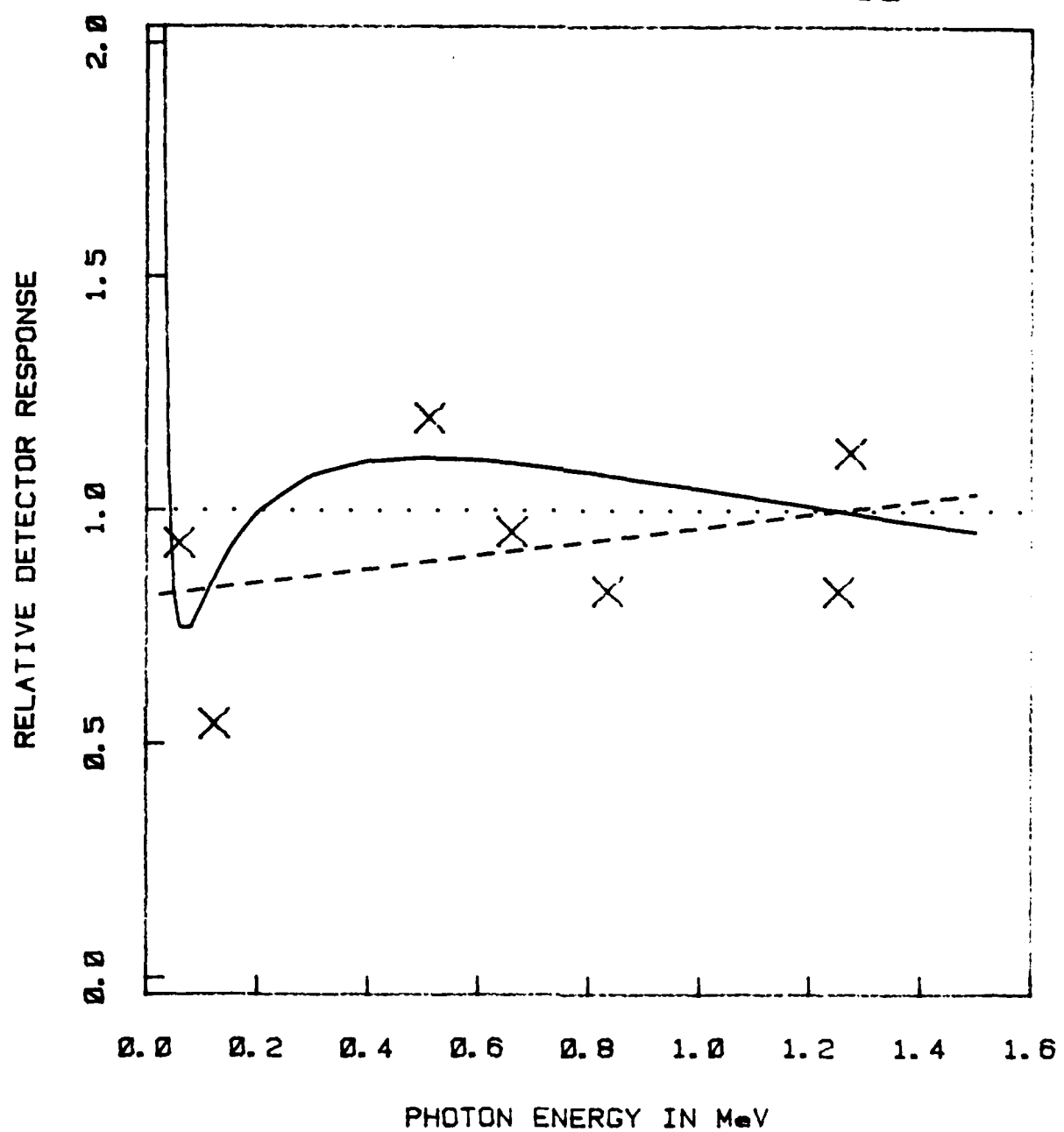


FIGURE 5. NPM54X Relative Detector Response Normalized to Cobalt 60. In this figure, the solid line is the polystyrene (C_8H_8) mass-energy absorption data (7:74); the dotted line is the flat response; and the dashed line is the linear regression response of the experimental data, which are the x's.

detector response chosen has very little effect upon the photon spectrum determined by DCON.

Filter Selection

The material available for the filters was Al, Cu, and Pb. The sizes that were available were 1/16 in. and larger in 1/16 in. increments for the Pb. For the Al, and Cu, 1/8 in. increments were available.

For the trial spectrum input into DCON, a two temperature exponentially decreasing spectrum was used. The two temperatures chosen were 10 and 50 keV, and were equally weighted. DCON was executed repeatedly using this spectra as input with the filters varied each time. It was found that the spectrum produced by DCON did not vary much (it was within 5%) from the input spectra in the interior of the energy mesh or bins. Near the endpoints of the mesh, the spectra output varied sometimes by as much as a factor of two or three. The worst of these results occurred when a different filter material was used on each detector. The best occurred when all the filters were of the same material. When the same material was used, the errors across the interior of the energy mesh being examined could be brought to within two or three percent and the error at the ends could be brought to within 20%. The smallest errors were achieved when the filter material was the same, the Z of the material was at or higher than that of steel, and the thicknesses of the filters varied by a factor of three from one detector to the next. Also, when using one of the detectors unfiltered, a requirement for the lowest filter size to

have a thickness of 1/8 in. or so was noticed for filters other than Pb. This is because the supposed "bare" detector is really already shielded by 3/8 in. of steel vacuum chamber, and 1/16 in. of Al or Cu does little additional attenuation.

The first sets of filters used did not take this information into account because they were being used to determine what size of detector signals could be expected from what filters. The data presented in the next section is from one of these shots. The detector serial numbers and filters used are listed in Table I.

Shot D6-4

The shot parameters and experimental data is listed in Table II. The signal from the two in. Pb filtered detector was zero, so the signals were input into the preprocessing program as shown. The deconvoluted spectrum is shown in Figure 6. The spectrum is plotted on a log-log plot. The linear portion of the spectrum extending from 35 keV to 100 keV demonstrates a spectral dependency upon the photon energy raised to some power over that region. There is also an interesting "bump" in the spectrum that is centered at about 500 keV. The neutron yield of the shot was 4.5×10^{17} . The total radiated power above 35 keV was 650 MW.

The spectrum shown in Figure 6 uses as input all of the detector responses listed in Table II except for the response from detector 079. For this shot, there were two detectors that were identically filtered with 1/8 in. of Cu (detectors 077 and 124). Figure 7 shows a comparison of the spectrum shown in Figure 6 and the spectrum computed when only one of the 1/8 in. Cu filtered

TABLE I.

Detector Filters For PUFF Shot D6-4

Detector Serial Number	Filter Material Thicknesses in CM				
	Fe	Air	Al	Cu	Pb
079-LV	0.9525	352.7	0.0	0.0	5.08
077-LV	0.9525	356.9	0.0	0.3175	0.0
123-LV	0.9525	358.8	0.635	0.3175	0.0
122-LV	0.9525	358.1	0.0	0.0	0.15875
124-LV	0.9525	359.7	0.0	0.3175	0.0
125-LV	0.9525	356.6	0.635	0.0	0.0

TABLE I. Detector Filters for PUFF shot D6-4. The Fe filter is the vacuum chamber wall. Note that detectors 077 and 123 have the same thickness of Cu filtration.

TABLE II.

Shot Data For PUFF Shot D6-4

Detector Serial Number	079-LV	077-LV	123-LV	122-LV	124-LV	125-LV
Detector Voltage	-0.0 V	-3.9	-5.0	-1.5	-5.0	-27.5
Error in Reading Trace	0.3 V	0.3	0.3	0.3	0.3	0.3
Filter Material	Pb	Cu	Al+Cu	Pb	Cu	Al
Detector Response Amps/(-Mev/Cm**2/Sec)	2.49E-10	1.88E-10	1.56E-10	1.41E-10	1.63E-10	1.62E-10

Detector Bias = -2800 V

First Minute Ag Neutron Activation Counts = n = 7662 Counts/Min

Ag Activation Counter Background = b = 160 Counts/Min

Neutron Yield = $0.6 \times 10^6 \exp(6) \times (n-b) = 4.5 \times 10^6 \exp(7)$

Bank Voltage = +/- 40,000 V

Lower Puffer Pressure = 900 psi

Upper Puffer Pressure = 0 (No upper Puff)

Total Radiated Power above 35 keV = $6.5 \times 10^6 \exp(8)$ watts

Table II. Shot Data for PUFF shot D6-4. The detector response listed is for ^{60}Co gamma radiation that was provided by the manufacturer.

PUFF Plasma Gun Spectrum Shot D6-4
Five Detector Signals Used

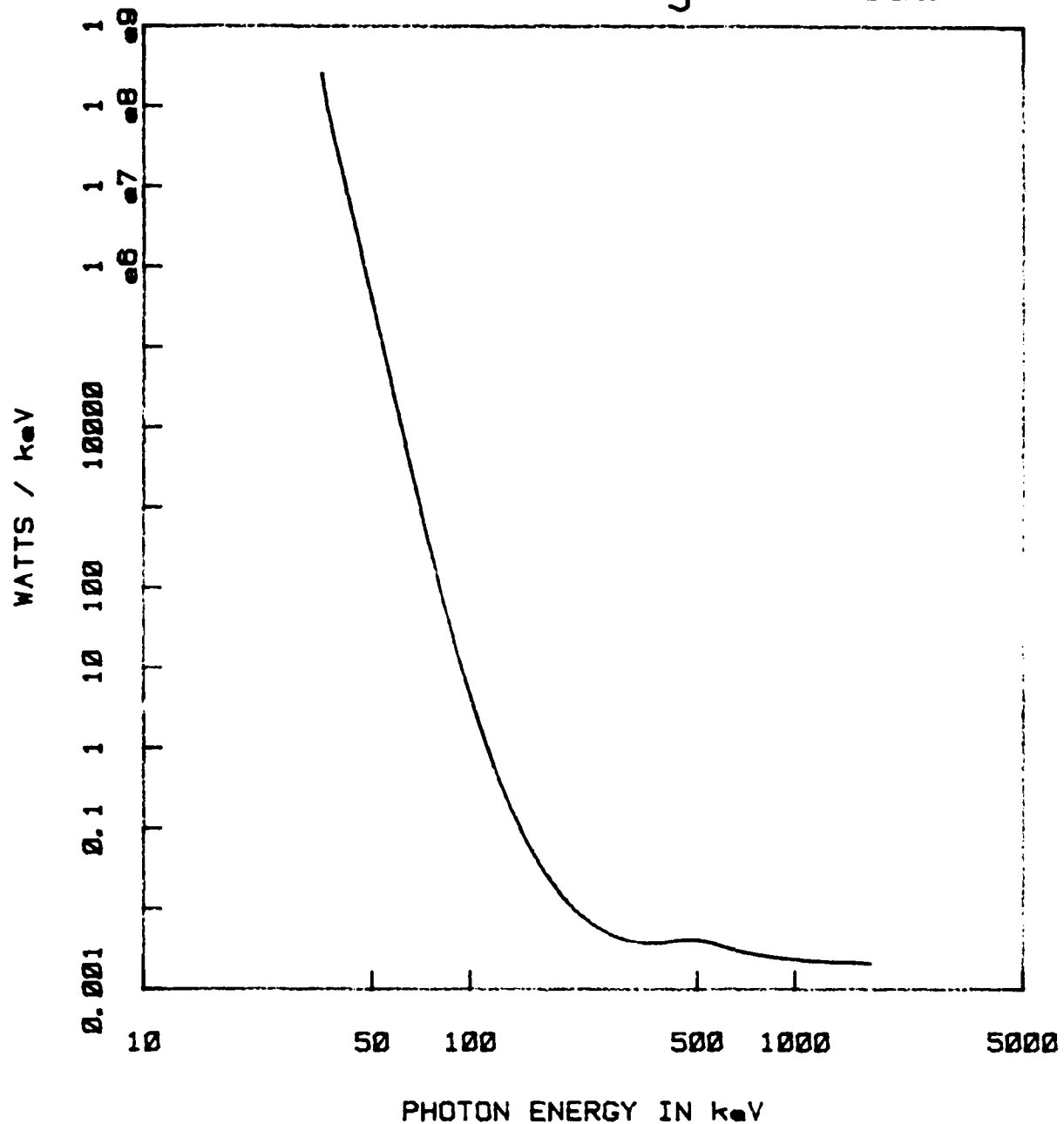


FIGURE 6. PUFF Plasma Gun Spectrum Shot D6-4 Five Detector Signals Used. This figure shows the results of the deconvolution of PUFF shot D6-4. All detector signals, except for the signal from detector 079 (filtered with 2 in. Pb) were used. The response function used was the C8H8 log-log interpolation.

PUFF Plasma Gun Spectrum Shot D6-4
Copper Filtered Detector Signals Varied

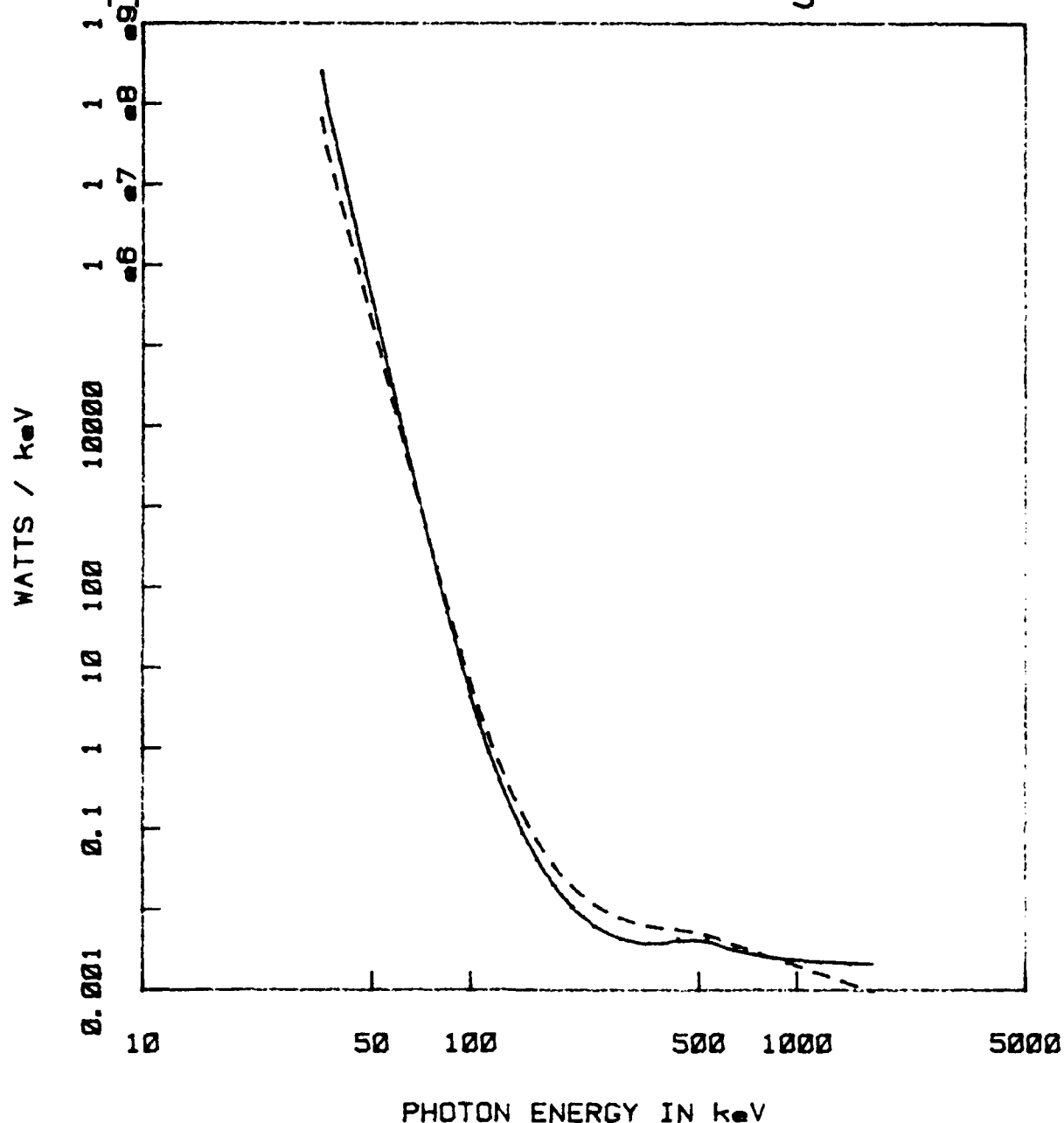


FIGURE 7. PUFF Plasma Gun Spectrum Shot D6-4 Copper Filtered Detector Signals Varied. The effects on the deconvolution of using only one signal from the two Cu filtered detectors (077 and 124) is shown. The solid line is the same spectrum as in Figure 6. The dotted line (hidden by the solid line) is from neglecting detector 077. The dashed line is from negelecting detector 124. The C8H3 response function was used in all three cases.

detectors is used as input. The solid line is the spectrum shown in Figure 6, the dotted line is the spectrum computed without the data from detector 124, and the dashed line is the spectrum computed without the data from detector 077.

As stated above, the spectrum in Figure 6 exhibits a power law dependency between 35 and 100 keV. The other two spectra shown in Figure 7 demonstrate this also. This power law dependency has the form

$$S = \beta(h\nu)^\alpha \quad (24)$$

where S is the spectra, beta is a constant determined from the height of the linear region at some arbitrary $(h\nu)$, $(h\nu)$ is the photon energy, and alpha is the slope of the linear region. Table III shows alpha's and beta's for the three spectra in addition to the alpha's and beta's for the spectra presented in Figure 8.

Figure 8 shows the effect of changing the absolute detector response. Again the solid line is the same spectrum shown in Figure 6. This spectrum was computed using the polystyrene mass energy absorption coefficients for the absolute detector response. The dashed spectrum was computed using the flat detector response. The dotted spectrum was computed using the linear regression detector response.

TABLE III.

Power Law Equation: $S = \beta(h\nu)^\alpha$

	Alpha	Beta
All Five Detectors:		
Polystyrene Detector Response	-17.024	$2.9895 \times 10^{-3} \exp(34)$
Flat Response	-17.020	$2.4272 \times 10^{-3} \exp(34)$
Linear Regression Response	-17.202	$6.9319 \times 10^{-3} \exp(34)$
Four Detectors:		
Detector 077 Excluded	-15.403	$2.957 \times 10^{-3} \exp(31)$
Detector 124 Excluded	-17.141	$5.316 \times 10^{-3} \exp(34)$

Table III. Parameters For Spectral Power Law Fit

PUFF Plasma Gun Spectrum Shot D6-4
Detector Response Function Varied

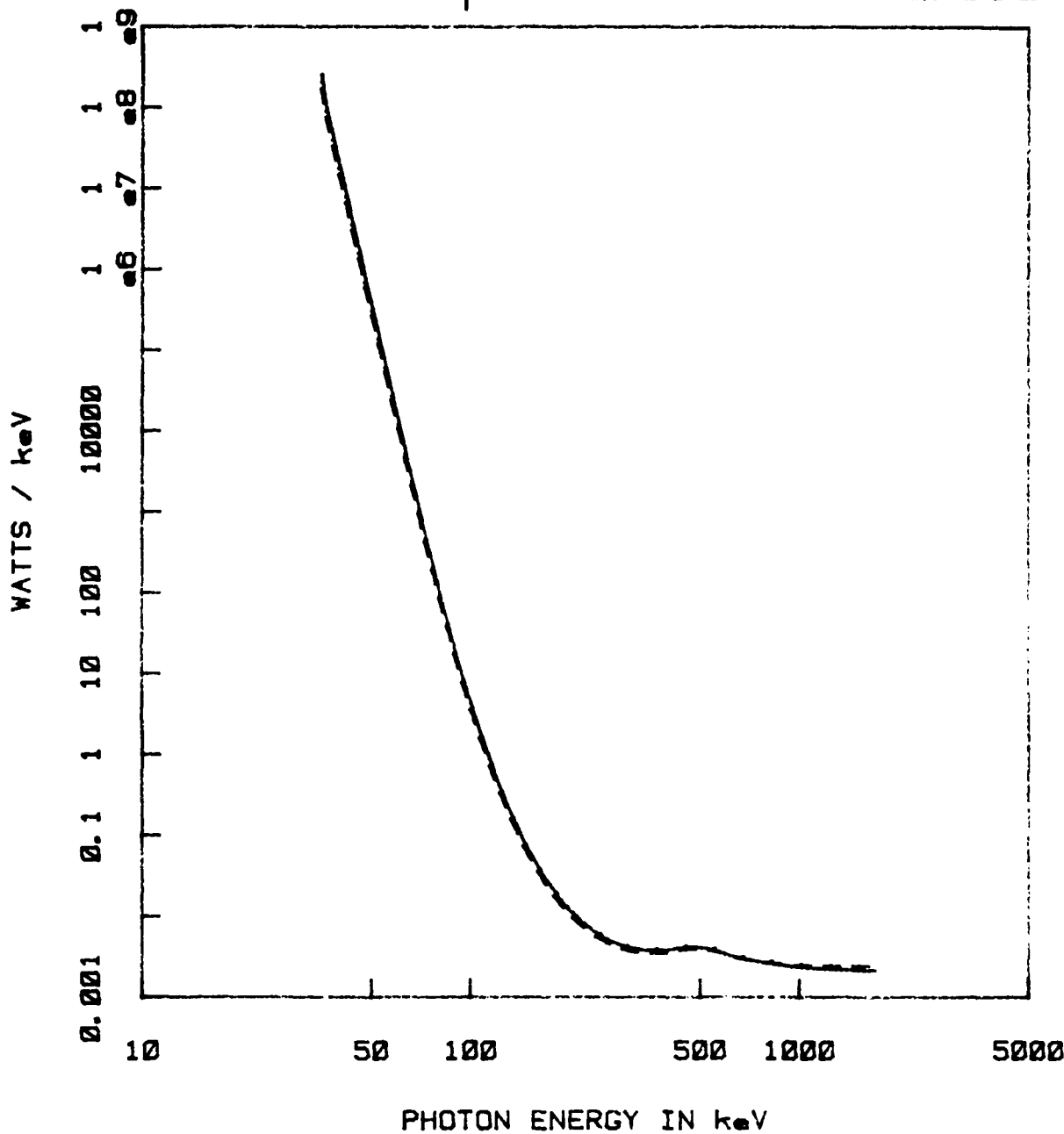


FIGURE 8. PUFF Plasma Gun Spectrum Shot D6-4 Detector Response Function Varied. This figure shows the effects of varying the relative detector response function in the program DCON. The solid line is the same spectrum as in Figure 6, and used the C8H8 response data. The dashed line used the flat response. The dotted line (hidden under the other two spectra) used the linear regression.

Experimental Errors

The sources of experimental errors and their estimated contributions are listed in Table IV. The contribution from the knowledge of the response functions of the detectors is definitely dominant. The contribution is 20% to a figure of 23% overall.

TABLE IV.

Type of Error	Contribution
Error in Reading Trace (Random)	about 3%
Error Due to EMP Change in Bias (Systematic)	about 1 to 2%
Error in Separating EMP Signal From Noise (Random)	0.05 to 1 V
Errors in Scope Calibration (Systematic)	about 1%
Errors in Distance Measurements (Systematic)	less than 0.5%
Error in Knowledge of Response Function (Unfiltered) (Systematic)	about +/- 20%
Error in Knowledge of Filter Transmissions (Systematic)	less than 5 to 10%
Total Error	about 23%

Table IV. List of Experimental Errors

VI. Conclusions And Discussion

Detector Calibration

Figure 5 on page 38 shows that the relative response for the detector was not determined very accurately. Therefore, besides the linear regression fit to the experimental calibration data, two other relative detector response functions were used. They were a flat response and a log-log fit to the mass energy absorption coefficients of polystyrene (C₈H₈). The polystyrene data from Hubble (7:74) was used because the response of the detector to various energy photons should vary as the mass energy absorption coefficients of the scintillating material varies. As was seen in Figure 8 though, changing the relative response function of the detectors changed the resulting spectrum very little. From this, it is reasonable to conclude further calibration of the detectors to photon energies is probably not necessary. However, it is recommended that the polystyrene data be used for the relative response because it should follow the actual detector responses closer than either the linear regression or the flat response.

Filter Selection

From the result section on filter selection, it would seem that Cu or Fe would make excellent filters. The problem with the Fe (or steel) was availability in a reasonable time frame. The Cu was available, but the problem was one the program DCON does not consider. The problem pertains to the detector signal

strength. The signals from the detectors need to be above one volt or so before the signal is above the electronic noise levels (usually about 50 mV) created by firing the bank. The detector signal should also not be above 20 or 25 volts, because the detector will then start to saturate and the response becomes nonlinear.

When using Cu as a filter material with 1/8 in. for the first filter and a factor of three increase of filter thickness from one detector to the next, there is no problem for the first two filter thicknesses (1/8 in. and 3/8 in.). For the next filter thickness, 9/8 in., the signal becomes too low. The dilemma raised is one of how to get various filters of the same material and varying thicknesses, but still get a reasonable signal. This was partially solved by first moving the unfiltered detector to a distance about twice as far away from the source as the other detectors. The filter "multiplication factor" was reduced to two, so three detectors were filtered with 1/8, 1/4, and 1/2 in. of Cu. With one detector dedicated to neutron detection (a two in. Pb filter), and seven detectors available, there were two detectors left that needed filters. Shot D6-4 demonstrated that 1/16 in. of Pb gave a reasonable signal, so that was used for the sixth detector. The seventh detector was then filtered with 1/2 in. of Al because it was available and it was hoped to produce a reasonable signal.

Shot D6-4

PUFF shot D6-4 produced a spectrum that is interesting in two aspects. The first aspect is the spectral output is a power law spectrum between 35 and 100 keV. It is not known by the author the exact significance of this result, but if bremsstrahlung is the major photon radiation production mechanism above 30 keV for PUFF with the coaxial rail gun, then the bremsstrahlung is probably produced by electrons whose energies are also distributed in a power law distribution between 35 and 100 keV.

The other interesting aspect is the small "feature" or "bump" in the spectrum at about 500 keV. The feature was originally thought to be a result of the type of iterative algorithm used because of the "end point error" problem discussed in the results section on filter selection. This was because the energy mesh was only extended up to 400 keV and the energy being radiated at the upper end of the spectrum was increasing. When the energy mesh was enlarged to the size seen, the increase turned out to not be the edge effect it was thought to be.

Figure 7 suggests this feature is due to an anomalous signal from detector 124. This is because the feature disappears when the signal from detector 124 is not included. This signal is anomalous because the signal from detector 124, which is shielded with 1/8 in. of Cu, is as large as the signal from detector 123, which is shielded with 1/4 in. of Al.

Probably the most important result is that the deconvoluted spectrum follows a power law, and the slope is changed by ignoring the anomalous detector signal.

Final Conclusions

Overall, the thesis seems to have been a successful one because a reasonable spectrum was produced by the method that was proposed. Therefore, the problem that was to be solved, that of devising a method to determine the high energy spectrum of SHIVA STAR, was accomplished. There were a few interesting results observed and discussed which hopefully point the way to further research. The only regret is that more time was not available for reducing the data available. It would be very interesting to have the current and voltage data analyzed so that one could check to see that the peak voltage is 100 kV or so the spectrum from shot D6-4 would indicate if the major photon production mechanism above 30 keV is bremsstrahlung. It would also be interesting to deconvolute more of the data. Over one hundred shots were performed, though many used a large magnetic probe array and only one scintillator photomultiplier detector. There also needs to be some further work done in the area of filter selection so that a better idea of an ideal filter set can be determined and used.

APPENDIX A

APPENDIX A

LISTING OF PROGRAM DCON

The following is a listing of the program DCON. As listed it will execute on a VAX 11/780 under the UNIX operating system. By changing the two OPEN statements in subroutine DATIN, the program will execute under the VMS operating system.

Sample input and output for the program are listed in Appendices B and C.

PROGRAM DCON

```

883 CALL SPCGEN
C continue
C Input observed signals. VO(I)=(1./50.)*(4.*PI/OMEGA)*(1./TMESH)*
C (VP OR INT(V*DT)) .VP in VOLTS for SPEC in WATTS/KEV,
C INT(V*DT) IN VOLT-SEC for SPEC in JOULES/keV
C
C CALL DETINP
IF ( IFLAG .EQ. 788 ) GOTO 799
C
C 902 / GOTO 902 is iteration/convergence loop...
C
902 CONTINUE
C
C Generate calculates detector signals...
C
C CALL CALDET
IF ( IFLAG .EQ. 903 ) GOTO 903
IF ( IFLAG .EQ. 904 ) GOTO 904
C
C Smoothing loop...
C
C CALL SMOOTH
C
C End of iteration/convergence loop...
C
GO TO 902
C
C
904 CONTINUE
C
C Convergence to specified max error ERMAX was not achieved...
C
WRITE(3,299)
299 FORMAT(1X,'//',*,          'ERROR .GT. ERMAX', // )
CONTINUE
WRITE(3,1001) IFLAG
C
C New output data that has been computed...
C
C CALL FINOUT
C
C Generate new initial spectrum?
C
IF ( NSPEC .EQ. 1 ) GOTO 460
C
C No, start from end of previous spectrum...
C
GOTO 803
799 CONTINUE
788 CONTINUE
C
C All finished, so close input and output files and stop...
C
CLOSE(UNIT=1)
WRITE(3,1002)
1002 FORMAT(1X,'*** COMPLETION OF COMPUTATION *** ', // )
FORMAT(1X,'*****', IFLAG=' ', 15 )
CLOSE(UNIT=3)
STOP
END

```



```

SUBROUTINE RESGEN
C
C This subroutine generates the 'bare' (unfiltered) NPM54X
C response function.
C
COMMON / ALL / TRES , NDET , KIT , KITMAX , E1 , RATIO ,
1 JLAST2(5) , X(15,12) , LMAT(5) , XMAT(5) , KDET(15) ,
2 VC(15) , VO(15) , NFILT(15) , MATNUM(15,15) ,
3 LABLE(2) , THING(5) , IT(3) , RESPBM(15) , CORPEC(15) ,
4 Z(12) , ECOEF(8,100) , COEF(8,100) , ERES(8,100) , PES(8,100) ,
5 EE(100) , XMU(8,100) , PCESPO(8,100) , FESP1(8,100) ,
6 DE(100) , SPEC(100) , DEL(15,15) , SO ,
7 CONV(100) , TSPEC(100) , SPEC2(100) , EPRNT(1000) ,
8 VCPRT(8,1000) , NSPEC , M ,
9 JJ1(125) , JJ2(125) , AREA(125) , WIDTH(125) , SBAP(125) ,
1 JBAR(125) , ISHOT , IDBUG , IFLAG , AA . BB , ND , NE , NP ,
2 KITP , GAMMA , ERROR , ERMAX ,
3 IDNUM(8) , DETCAL(8) , ISNUM(8) , DSTCAL(8)

Detector serial numbers...
DATA ISNUM / 077 , 078 , 079 , 080 ,
1 122 , 123 , 124 , 125 /
Detector response in Amps/(Gamma-MeV/CM**2/SEC)
DATA DSTCAL / 1.88E-10 , 2.00E-10 , 2.49E-10 , 1.71E-10 ,
1 1.41E-10 , 1.56E-10 , 1.01E-10 , 1.62E-10 .
Change DSTCAL to keV (multiply by 1 = 1 Mev . 1000 kev)...
IFLAG = 1
DO 400 I = 1 , 8
DSTCAL(I) = 0.001 * DSTCAL(I)
400 CONTINUE
Determine who belongs to who in a detector sort...
DO 300 I = 1 , NDET
J = 0
250 CONTINUE
J = J + 1
IF ( J .GE. 9 ) GOTO 9999
IF ( IDNUM(I) .NE. ISNUM(J) ) GOTO 250
DETCAL(I) = DSTCAL(J)
300 CONTINUE
M = NE - 1
EE(1)= E1
FESCAL is relative calibration normalization factor...6000=1.0...
VCAL is a function that returns a detector response that needs
to be normalized...
RESCAL = VCAL(1253.0,IFLAG)
IF ( !IFLAG .EQ. -1 ) GOTO 9999
DO 100 J = 1 , NE
IF ( J .NE. 1 ) EE(J) = EE( J - 1 ) * RATIO
100 CONTINUE
Calculate relative calibration factor PES1...

```

```
RES1 = VCAL(EE(J),IFLAG)
IF ( IFLAG .EQ. -1 ) GOTO 9999
C
C Normalize relative calibration factor...
C
RES1 = RES1 / RESCAL
DO 50 I = 1 , NDET
C
C RES(I,J) is response of the I'th detector at the energy
C ERES(I,J).
C
C ERES(I,J) is energy in keV. RES(I,J) is 'bare' (unfiltered)
C NPM54X responses in ...
C
RES(I,J) = RES1 * DETCAL(I)
RESPO(I,J) = RES(I,J)
ERES(I,J) = EE(J)
50  CONTINUE
100  CONTINUE
RETURN
9999  CONTINUE
IFLAG = -3
RETURN
END
```



```
1      IF ( E .LT. EVCAL(1) ) GOTO 9999
CONTINUE
IF ( E .LT. EVCAL(J) ) GOTO 2
C
C      Test for out of bounds...
C
IF ( J .GE. 26 ) GOTO 9999
J = J + 1
GOTO 1
CONTINUE
2      JM1 = J - 1
ENGTOP = ALOG( EVCAL(J) )
ENGBOT = ALOG( EVCAL(JM1) )
RHOTOP = ALOG( RVCAL(J) )
RHOBOT = ALOG( RVCAL(JM1) )
ENGL = ALOG( E ) - ENGBOT
SLOPE = ( RHOTOP - RHOBOT ) / ( ENGTOP - ENGBOT )
VCAL = RHOBOT + ENGL * SLOPE
VCAL = EXP( VCAL )
RETURN
9999  CONTINUE
IFLAG = -1
RETURN
END
```

```

SUBROUTINE FINOUT
C
C This subroutine outputs the computed spectrum when the technique C
C either converges or fails to converge. C
C
C
C
COMMON / ALL / TRES , NDET , KIT , KITMAX , E1 , RATIO ,
1 JLAST2(5) , X(15,12) , LMAT(5) , XMAT(5) , KDET(15) ,
2 VC(15) , VO(15) , NFILT(15) , MATNUM(15,15) ,
3 LABLE(2) , THING(5) , IT(3) , RESPSC(15) , CORREC(15) ,
4 Z(12) , ECOEF(8,100) , COEF(8,100) , ERES(8,100) , RES(8,100) ,
5 EE(100) , XMU(8,100) , RESPO(8,100) , RESPI(8,100) ,
6 DE(100) , SPEC(100) , DEL(15,15) , SO .
7 CONV(100) , TSPEC(100) , SPEC2(100) , EPRNT(1000) ,
8 VCPRT(8,1000) , NSPEC , M ,
9 JJ1(125) , JJ2(125) , AREA(125) , WIDTH(125) , SBAR(125) ,
1 JBAR(125) , ISHOT , IDBUG , IFLAG , AA , BB , ND , NE , NP ,
2 KITP , GAMMA , ERROR , EPMAX ,
3 IDNUM(8) , DETCAL(8) , ISNUM(8) , DSTCAL(8)
ITCC = 0
LL2 = 12
IF ( NDET .LE. 12) LL2 = NDET
350 CONTINUE
WRITE(3,351) ( K , K = 1 , LL2 )
351 FORMAT( // , 1X , 'K' , 'ERROR(K)' , 17 , 1I10 , // )
352 FORMAT( // , 1X , 'K' , , 3I10 , // )
WRITE(3,891)
891 FORMAT( 1X , // )
DO 556 K = 1 , KITP
WPITE(3,303) K , EPRNT(K) , ( VCPRT(I,K) , I = 1 , LL2 )
556 CONTINUE
IF ( NDET .LE. 12 ) GOTO 354
WRITE(3,352) ( I , I = 13 , NDET )
WRITE(3,891)
DO 557 I = 1 , KITP
WPITE(3,353) I , ( VCPRT(I,I) , I = 13 , NDET )
557 CONTINUE
353 FORMAT( 1X , 15 , 3E10.3 )
354 FORMAT( 1X , 15 , 13E10.3 )
CONTINUE
WRITE(3,297)
297 FORMAT( 1H0 , // , 4X , 'DET' , 7X , 'ODS. SIGNAL' ,
1 8X , 'CALC. SIGNAL' , // )
DO 56 I = 1 , NDET
WRITE(3,296) I , VO(I) , VC(I)
FORMAT( 1X , 15 , 4X , E5.4 , 5X , E15.4 )
56 CONTINUE
SSPEC = 0.0E0
DO 54 J = 1 , NE
SSPEC = SSPEC + SPEC(J) * DE(J)
TSPEC(J) = SSPEC
54 CONTINUE
WPITE(3,304)
304 FORMAT( // , 1X , 'EE(J) (keV)' , 5X , 'SPEC(J)' ,
1 ' (Watts/keV)' , 3X ,
1 ' TSPEC(J) (Watts)' , // )
DO 114 J = 1 , NE
C
C Change from Watts/Joule to Watts/keV...
C
SPEC(J) = SPEC(J) * 1.6E-16

```

TSPEC(J) = TSPEC(J) * 1.602E-16
305 WRITE(3,305) EE(J), SPEC(J), TSPEC(J)
114 FORMAT(1X, F18.4, 2E20.4)
CONTINUE
RETURN
END


```

52  CONTINUE
C
C Divide by number of detectors NDET to get error per detector...
C
C ERROR = ERROR / DFLOAT(NDET)
C
C Store error, iteration number -vs- detector
C
EPRNT(KIT) = ERROR
DO 519 I = 1 , NDET
VCPRNT(I,KIT) = VC(I)
519
CONTINUE
KITP = KIT
C
C KIT is number of iterations. At end of present iteration,
C so increment by one...
C
KIT = KIT + 1
C
Check for convergence...
C
IF ( ERROR .LT. ERMAX ) GOTO 903
C
Check to see if iteration limit KITMAX has been reached...
C
IF ( KIT .GT. KITMAX ) GOTO 904
C
Have not reached error or iteration limits,
C so ...
C
DO 108 J = 1 , NE
SUM1 = 0.0E0
SUM2 = 0.0E0
DO 109 I = 1 , NDET
SUM1 = SUM1 + ( RESPI(I,J) / RESPSM(I) ) * CORREC(I)
SUM2 = SUM2 + ( RESPI(I,J) / RESPSM(I) )
109
CONTINUE
XCONV = 0.0E0
IF ( SUM1 .EQ. 0.0E0 ) GOTO 120
XCONV = ALOG(SUM1) - ALOG(SUM2)
120
CONTINUE
IF ( XCONV .LT. -82.89E0 ) XCONV = -82.89E0
IF ( XCONV .GT. 82.89E0 ) XCONV = 82.89E0
XTEMP = ALOG( SPEC(J) ) + XCONV
IF ( XTEMP .LT. -82.89E0 ) XTEMP = -82.89E0
IF ( XTEMP .GT. 82.89E0 ) XTEMP = 82.89E0
SPEC(J) = EXP(XTEMP)
IF ( SPEC(J) .LT. 1.0E-30 ) SPEC(J) = 1.0E-36
108
CONTINUE
RETURN
903
CONTINUE
C
Have achieved specified convergence, so ...
C
IFLAG = 903
RETURN
904
CONTINUE
C
Have reached iteration limit...
C
IFLAG = 904
RETURN
END

```



```

XBAR = ( ALOG ( EBAR / EE(L1) ) / ALOG(RATIO) )
JBAR(N) = L1 + INT(XBAR)
1202 CONTINUE
DO 1200 N = 1 , NMAX
SPEC2( JBAR(N) ) = SBAR(N)
1200 CONTINUE
C
SPEC2(1) = SPEC(1)
SPEC2(NE) = SPEC(NE)
KMAX = NMAX
DO 1204 K = 1 , KMAX
K1 = 1
K2 = NE
IF ( K .NE. 1 ) K1 = JBAR(K-1)
IF ( K .NE. KMAX ) K2 = JBAR(K)
DO 1205 J = K1 , K2
XTEMP = ALOG( SPEC2(K1) ) + ( ALOG( SPEC2(K2) ) -
1           ALOG( SPEC2(K1) ) )
2           * ( ALOG( EE(J) ) - ALOG( EE(K1) ) ) /
3           ( ALOG( EE(K2) ) - ALOG( EE(K1) ) )
IF ( XTEMP .LT. -82.89E0 ) XTEMP = -82.89E0
IF ( XTEMP .GT. 82.89E0 ) XTEMP = 82.89E0
SPEC2(J) = EXP(XTEMP)
1205 CONTINUE
1204 CONTINUE
DO 1206 J = 1 , NE
SPEC(J) = SPEC2(J)
1206 CONTINUE
1107 CONTINUE
RETURN
END

```



```
C
3      CONTINUE
C      XMU(I,J) is the sumation of all the cross sections of all
C      the filters for detector I at energy ENG...
C
5      XMU(I,J) = SUM
CONTINUE
DO 10 I = 1 , NDET
DO 10 J = 1 , NE
C
C      RESP1(I,J) is the response of detector I at energy EE(J)...
C
10    RESP1(I,J) = RESPO(I,J) * EXP( - XMU(I,J) )
CONTINUE
DO 102 I = 1 , NDET
RSUM = 0.0E0
DO 101 J = 1 , M
RSUM = RSUM + 0.5E0 * ( RESP1(I,J) + RESP1( I , J + 1 ) ) * DE(J)
101  CONTINUE
RESPSM(I) = RSUM
102  CONTINUE
CALL BEGOUT
RETURN
999  CONTINUE
IFLAG = 799
RETURN
END
```

```

SUBROUTINE CROSS(MAT,ENG,CRO,DEL,IFLAG,IDBUG)
DIMENSION DENSTY(5)
DATA JFLAG / 1 /
C
C Material densities in gm/cm**3
C
DATA DENSTY / 11.05E0 , 2.6989E0 , 7.874E0 ,
1           8.96E0 , 1.29E-3 /
C
C Convert air density to altitude in Albuquerque (83% of sea-level)
C
IF ( JFLAG .EQ. 1 ) DENSTY(5) = DENSTY(5) * 0.83E0
JFLAG = JFLAG + 1
C
C Get RHO, which is the cross section of material MAT in gm/cm**2
C at energy ENG which is in keV.
C
CALL CSECT(MAT,ENG,RHO,IFLAG,IDBUG)
C
C If IFLAG = -1, then cross section was not computed, so exit...
C
IF ( IFLAG .EQ. -1 ) GOTO 9999
C
C CRO is unitless, and is the density of the filter (DENSTY) in
C gm/cm**3 times the thickness of the filter (DEL) in cm times
C the material cross section (RHO) in cm**2/gm
C
CRO = DENSTY(MAT) * DEL * RHO
RETURN
9999 CONTINUE
WRITE(6,9998) MAT , ENG
9998 FORMAT(' IFLAG = -1, MAT=',I2,' ENG=',E16.8)
STOP
END

```


3 9.54E-2 , 8.70E-2 , 8.05E-2 , 7.07E-2 , 6.36E-2 , 5.10E-2 ,
4 4.45E-2 , 3.58E-2 , 3.08E-2 , 2.75E-2 , 8 * 0.0 /

C
C Table energies in Mev
C

C DATA ENERG1 /

C C Lead

1 1.00E-2 , 1.30E-2 , 1.50E-2 , 1.52E-2 , 1.52E-2 , 1.59E-2 ,
2 1.59E-2 , 1.59E-2 , 2.00E-2 , 3.00E-2 , 4.00E-2 , 5.00E-2 ,
3 6.00E-2 , 8.00E-2 , 8.00E-2 , 8.80E-2 , 1.00E-1 , 1.50E-1 ,
4 2.00E-1 , 3.00E-1 , 4.00E-1 , 5.00E-1 , 6.00E-1 , 8.00E-1 ,
5 1.00E+0 , 1.50E+0 , 2.00E+0 , 3.00E+0 , 4.00E+0 , 5.00E+0 ,

C C Aluminum, MAT = 2

1 1.00E-2 , 1.50E-2 , 2.00E-2 , 3.00E-2 , 4.00E-2 , 5.00E-2 ,
2 6.00E-2 , 8.00E-2 , 1.00E-1 , 1.50E-1 , 2.00E-1 , 3.00E-1 ,
3 4.00E-1 , 5.00E-1 , 6.00E-1 , 8.00E-1 , 1.00E+0 , 1.50E+0 ,
4 2.00E+0 , 3.00E+0 , 4.00E+0 , 5.00E+0 , 8 * 0.0 /

C C Iron, MAT = 3

C DATA ENERG2 /

1 1.00E-2 , 1.50E-2 , 2.00E-2 , 3.00E-2 , 4.00E-2 , 5.00E-2 ,
2 6.00E-2 , 8.00E-2 , 1.00E-1 , 1.50E-1 , 2.00E-1 , 3.00E-1 ,
3 4.00E-1 , 5.00E-1 , 6.00E-1 , 8.00E-1 , 1.00E+0 , 1.50E+0 ,
4 2.00E+0 , 3.00E+0 , 4.00E+0 , 5.00E+0 , 8 * 0.0 ,

C C Copper, MAT = 4

1 1.00E-2 , 1.50E-2 , 2.00E-2 , 3.00E-2 , 4.00E-2 , 5.00E-2 ,
2 6.00E-2 , 8.00E-2 , 1.00E-1 , 1.50E-1 , 2.00E-1 , 3.00E-1 ,
3 4.00E-1 , 5.00E-1 , 6.00E-1 , 8.00E-1 , 1.00E+0 , 1.50E+0 ,
4 2.00E+0 , 3.00E+0 , 4.00E+0 , 5.00E+0 , 8 * 0.0 ,

C C Air, MAT = 5

1 1.00E-2 , 1.50E-2 , 2.00E-2 , 3.00E-2 , 4.00E-2 , 5.00E-2 ,
2 6.00E-2 , 8.00E-2 , 1.00E-1 , 1.50E-1 , 2.00E-1 , 3.00E-1 ,
3 4.00E-1 , 5.00E-1 , 6.00E-1 , 8.00E-1 , 1.00E+0 , 1.50E+0 ,
4 2.00E+0 , 3.00E+0 , 4.00E+0 , 5.00E+0 , 8 * 0.0 /

DATA GAMMA / 1.2E0 /

RETURN

END


```

7   FORMAT( 1H1 , 25X , ' BEGIN NPM54X SPECTRUM UNFOLD CODE' , // )
C
C   Read in how many detectors were used...
C
10  READ(1,10) NDET
C   FORMAT(I2)
C
C   Loop over the number of detectors
C
DO 100 I = 1 , NDET
C
C   Read in detector serial numbers...
C
12  READ(1,12) IDNUM(I)
C   FORMAT(I3)
C
C   Read number of filters used for detector I...
C
READ(1,10) NFILT(I)
C
C   Loop over the number of filters for detector I...
C
DO 20 J = 1 , NFILT(I)
C
C   Read in material number and thickness in centimeters for
C   filter J of detector I...
C
15  READ(1,15) MATNUM(I,J) , DEL(I,J)
C   FORMAT(I1,E16.8)
20  CONTINUE
100 CONTINUE
C
C   Input initial spectrum, iteration/convergence parameters
C
READ(1,200) SO , NP , EPMAX , KITMAX , NSPEC , T1 , T2
C
C   SO is value for initial flat spectrum, if < 0 then
C   two temperature exponential is used instead.
C   NP is
C   ERMAX is average error allowed per detector for the
C   completion of the convergence
C   KITMAX is the maximum number of iterations allowed
C   T1 and T2 are the temperatures to be used for the
C   two temperature exponential initial iteration
C
200 FORMAT( E16.8 , I5 , E16.8 , 2I5 , 2E16.8 )
WRITE(3,210) NDET , SO , NP , NSPEC , ERMAX , T1 , T2
210 FORMAT( 1H0 , // , 1X , 'ND=' , I5 , / , 1X , 'SO=' , E14.4 , / ,
1      '1X , 'NP=' , I5 , 'NSPEC=' , I2 , / , 1X ,
2      'ERMAX=' , E11.4 , / , 1X ,
3      'T1=' , E16.8 , ' keV ' , 'T2=' , E16.8 , ' keV ' , // )
C
C   Input energy limits/number of groups/etc...
C
READ(1,220) NE , E1 , PATIO , AA , BB
220 FORMAT(I5.4E16.8)
WRITE(3,230) NE , E1 , PATIO , AA , BB
230 FORMAT( 'NE=' , I5 , 'PATIO=' , E16.8 , ' keV ' , 'E2=' , E16.8 ,
1      'AA=' , E16.8 , 'BB=' , E16.8 )
RETURN
CONTINUE
IFLAG = -2
END

```

APPENDIX B

Appendix B

Sample Input for Program DCON

The listing on the next page is sample input for the program DCON. This input was generated by the program PIN, which is listed in Appendix D. The input for program PIN to generate this data is listed in Appendix E. Using this data as input for program DCON will generate the output listed in Appendix C.

684	
5	
125	
3	.95249999e+00
3	.95249999e+00
5	.36555200e+03
2	.63499999e+00
77	
3	
3	.95249999e+00
5	.35687000e+03
4	.31750000e+00
122	
3	
3	.95249999e+00
5	.35014001e+03
1	.15075000e+00
123	
4	
3	.95249999e+00
5	.35077499e+03
4	.31750000e+00
2	.63499999e+00
124	
3	
3	.95249999e+00
5	.35272751e+03
4	.31750000e+00
1	.10000000e+01
100	
3	.25000000e+02
100	.3920e+15,

.0000000e+00

APPENDIX C

APPENDIX C

Sample Output for Program DCON

This is a listing of sample output generated by program DCON. This output was generated by using the sample input data listed in Appendix B.

BEGIN NPM54X SPECTRUM UNFOLD CODE

ND= 5
 SO= .1000e+01
 NP= 1 NSPEC= 1
 ERMAX= .1000e-05
 T1= .00000000e+00 keV T2= .00000000e+00 keV

NE= 100 RATIO= .35000000e+02 keV E2= .10400000e+01

ISHOT 604 AA= .00000000e+00 BB= .00000000e+00

RESPONSE IN VOLTS/Joule

DETECTOR	1	2	3	4	5
E(keV)					
.350e+02	.390e-30	.296e-36	.000e+00	.000e+00	.000e+00
.364e+02	.251e-26	.137e-35	.000e+00	.336e-36	.118e-35
.379e+02	.104e-26	.330e-33	.000e+00	.905e-34	.286e-33
.394e+02	.289e-25	.446e-31	.263e-36	.135e-31	.387e-31
.409e+02	.564e-24	.364e-29	.615e-34	.119e-29	.315e-29
.426e+02	.807e-23	.188e-27	.832e-32	.660e-22	.163e-27
.443e+02	.873e-22	.644e-26	.682e-30	.240e-26	.558e-26
.461e+02	.735e-21	.152e-24	.357e-28	.600e-25	.131e-24
.479e+02	.495e-20	.256e-23	.125e-26	.107e-23	.222e-23
.498e+02	.272e-19	.321e-22	.303e-25	.141e-22	.278e-22
.518e+02	.118e-18	.282e-21	.499e-24	.128e-21	.244e-21
.539e+02	.439e-18	.197e-20	.620e-23	.931e-21	.171e-20
.560e+02	.144e-17	.114e-19	.602e-22	.556e-20	.988e-20
.583e+02	.418e-17	.553e-19	.467e-21	.278e-19	.479e-19
.606e+02	.108e-16	.226e-18	.292e-20	.117e-18	.196e-18
.630e+02	.246e-16	.777e-18	.148e-19	.409e-18	.673e-18
.656e+02	.519e-16	.238e-17	.641e-19	.128e-17	.206e-17
.682e+02	.103e-15	.656e-17	.243e-18	.359e-17	.569e-17
.709e+02	.191e-15	.165e-16	.812e-18	.918e-17	.143e-16
.737e+02	.335e-15	.380e-16	.242e-17	.215e-16	.329e-16
.767e+02	.561e-15	.811e-16	.654e-17	.467e-16	.703e-16
.798e+02	.895e-15	.161e-15	.161e-16	.943e-16	.140e-15
.829e+02	.132e-14	.285e-15	.349e-16	.168e-15	.247e-15
.863e+02	.187e-14	.478e-15	.707e-16	.286e-15	.414e-15
.897e+02	.260e-14	.770e-15	.871e-16	.464e-15	.667e-15
.933e+02	.351e-14	.119e-14	.388e-19	.726e-15	.103e-14
.970e+02	.464e-14	.173e-14	.151e-18	.110e-14	.155e-14
.101e+03	.592e-14	.250e-14	.511e-18	.157e-14	.220e-14
.105e+03	.711e-14	.330e-14	.148e-17	.206e-14	.266e-14
.109e+03	.845e-14	.424e-14	.389e-17	.266e-14	.367e-14
.114e+03	.990e-14	.535e-14	.944e-17	.328e-14	.464e-14
.118e+03	.116e-13	.608e-14	.212e-16	.403e-14	.579e-14
.123e+03	.135e-13	.820e-14	.444e-16	.524e-14	.712e-14
.126e+03	.155e-13	.999e-14	.874e-16	.641e-14	.866e-14
.133e+03	.177e-13	.120e-13	.162e-15	.774e-14	.104e-13
.138e+03	.200e-13	.140e-13	.286e-15	.920e-14	.124e-13
.144e+03	.226e-13	.160e-13	.481e-15	.110e-13	.146e-13
.149e+03	.253e-13	.196e-13	.773e-15	.129e-13	.170e-13
.155e+03	.273e-13	.218e-13	.115e-14	.143e-13	.189e-13

.162e+03	.293e-13	.240e-13	.164e-14	.158e-13	.208e-13
.168e+03	.314e-13	.263e-13	.229e-14	.174e-13	.228e-13
.175e+03	.336e-13	.288e-13	.311e-14	.191e-13	.249e-13
.182e+03	.359e-13	.314e-13	.412e-14	.209e-13	.272e-13
.189e+03	.382e-13	.341e-13	.534e-14	.228e-13	.295e-13
.197e+03	.406e-13	.369e-13	.679e-14	.248e-13	.320e-13
.204e+03	.427e-13	.393e-13	.835e-14	.265e-13	.341e-13
.213e+03	.444e-13	.414e-13	.998e-14	.280e-13	.359e-13
.221e+03	.462e-13	.435e-13	.118e-13	.295e-13	.377e-13
.230e+03	.481e-13	.457e-13	.138e-13	.311e-13	.396e-13
.239e+03	.499e-13	.480e-13	.159e-13	.327e-13	.416e-13
.249e+03	.518e-13	.502e-13	.182e-13	.344e-13	.436e-13
.259e+03	.537e-13	.526e-13	.206e-13	.361e-13	.456e-13
.269e+03	.557e-13	.550e-13	.231e-13	.379e-13	.477e-13
.280e+03	.577e-13	.574e-13	.258e-13	.397e-13	.498e-13
.291e+03	.597e-13	.599e-13	.286e-13	.415e-13	.519e-13
.303e+03	.616e-13	.623e-13	.313e-13	.433e-13	.540e-13
.315e+03	.632e-13	.641e-13	.338e-13	.447e-13	.556e-13
.327e+03	.647e-13	.660e-13	.362e-13	.461e-13	.572e-13
.340e+03	.663e-13	.679e-13	.387e-13	.475e-13	.588e-13
.354e+03	.678e-13	.698e-13	.412e-13	.490e-13	.605e-13
.368e+03	.694e-13	.717e-13	.437e-13	.505e-13	.621e-13
.383e+03	.710e-13	.736e-13	.462e-13	.520e-13	.638e-13
.398e+03	.726e-13	.756e-13	.487e-13	.535e-13	.655e-13
.414e+03	.801e-13	.772e-13	.508e-13	.593e-13	.669e-13
.431e+03	.849e-13	.788e-13	.529e-13	.632e-13	.683e-13
.448e+03	.878e-13	.804e-13	.549e-13	.658e-13	.697e-13
.466e+03	.899e-13	.821e-13	.569e-13	.676e-13	.711e-13
.485e+03	.915e-13	.837e-13	.589e-13	.692e-13	.725e-13
.504e+03	.929e-13	.853e-13	.608e-13	.706e-13	.739e-13
.524e+03	.937e-13	.866e-13	.625e-13	.715e-13	.751e-13
.545e+03	.940e-13	.880e-13	.641e-13	.721e-13	.763e-13
.567e+03	.931e-13	.894e-13	.657e-13	.718e-13	.775e-13
.589e+03	.892e-13	.908e-13	.672e-13	.691e-13	.787e-13
.613e+03	.860e-13	.920e-13	.687e-13	.669e-13	.798e-13
.638e+03	.870e-13	.933e-13	.700e-13	.679e-13	.808e-13
.663e+03	.880e-13	.945e-13	.713e-13	.690e-13	.819e-13
.690e+03	.888e-13	.955e-13	.725e-13	.699e-13	.828e-13
.717e+03	.896e-13	.965e-13	.736e-13	.708e-13	.837e-13
.746e+03	.904e-13	.976e-13	.747e-13	.717e-13	.846e-13
.776e+03	.912e-13	.986e-13	.758e-13	.726e-13	.855e-13
.807e+03	.919e-13	.995e-13	.768e-13	.735e-13	.863e-13
.839e+03	.926e-13	.100e-12	.776e-13	.742e-13	.870e-13
.873e+03	.931e-13	.101e-12	.784e-13	.750e-13	.876e-13
.907e+03	.937e-13	.102e-12	.792e-13	.757e-13	.883e-13
.944e+03	.943e-13	.103e-12	.799e-13	.764e-13	.889e-13
.982e+03	.948e-13	.103e-12	.806e-13	.771e-13	.896e-13
.102e+04	.952e-13	.104e-12	.811e-13	.777e-13	.901e-13
.106e+04	.956e-13	.104e-12	.816e-13	.782e-13	.905e-13
.110e+04	.959e-13	.105e-12	.820e-13	.788e-13	.909e-13
.115e+04	.962e-13	.105e-12	.824e-13	.793e-13	.913e-13
.119e+04	.964e-13	.106e-12	.827e-13	.797e-13	.917e-13
.124e+04	.966e-13	.106e-12	.830e-13	.801e-13	.919e-13
.129e+04	.967e-13	.106e-12	.831e-13	.804e-13	.921e-13
.134e+04	.967e-13	.106e-12	.833e-13	.806e-13	.922e-13
.140e+04	.967e-13	.106e-12	.834e-13	.808e-13	.923e-13
.145e+04	.966e-13	.107e-12	.834e-13	.810e-13	.924e-13
.151e+04	.966e-13	.107e-12	.834e-13	.812e-13	.924e-13
.157e+04	.963e-13	.106e-12	.832e-13	.812e-13	.922e-13
.163e+04	.960e-13	.106e-12	.830e-13	.811e-13	.920e-13
.170e+04	.958e-13	.106e-12	.827e-13	.811e-13	.918e-13
	.3920e+05		.5300e+04	.2051e+04	.6680e+04

.6899e+04

.00000e+00

ERROR .GT. ERMAX

***** IFLAG= 984 *****

K	ERROR(K)	1	2	3	4	5
1	.188e+01	.136e-09	.144e-09	.106e-09	.108e-09	.125e-09
2	.344e+07	.902e+07	.952e+07	.693e+07	.714e+07	.825e+07
3	.318e+00	.394e+04	.413e+04	.296e+04	.309e+04	.358e+04
4	.863e+01	.188e+05	.195e+05	.137e+05	.146e+05	.169e+05
5	.342e+01	.135e+05	.138e+05	.953e+04	.103e+05	.120e+05
6	.427e+01	.155e+05	.155e+05	.102e+05	.115e+05	.134e+05
7	.367e+01	.161e+05	.153e+05	.949e+04	.112e+05	.133e+05
8	.319e+01	.177e+05	.156e+05	.670e+04	.113e+05	.135e+05
9	.253e+01	.201e+05	.159e+05	.749e+04	.113e+05	.137e+05
10	.133e+01	.198e+05	.138e+05	.566e+04	.966e+04	.120e+05
11	.172e+01	.282e+05	.168e+05	.505e+04	.114e+05	.146e+05
12	.123e+01	.308e+05	.162e+05	.344e+04	.107e+05	.141e+05
13	.116e+01	.336e+05	.163e+05	.250e+04	.106e+05	.141e+05
14	.113e+01	.351e+05	.162e+05	.191e+04	.105e+05	.141e+05
15	.405e+00	.275e+05	.119e+05	.136e+04	.764e+04	.103e+05
16	.139e+01	.409e+05	.173e+05	.160e+04	.110e+05	.150e+05
17	.109e+01	.380e+05	.160e+05	.129e+04	.101e+05	.138e+05
18	.114e+01	.386e+05	.162e+05	.120e+04	.103e+05	.140e+05
19	.114e+01	.384e+05	.162e+05	.113e+04	.102e+05	.140e+05
20	.397e+00	.286e+05	.116e+05	.913e+03	.732e+04	.100e+05
21	.143e+01	.432e+05	.174e+05	.124e+04	.110e+05	.151e+05
22	.109e+01	.392e+05	.159e+05	.108e+04	.101e+05	.138e+05
23	.115e+01	.396e+05	.162e+05	.106e+04	.102e+05	.140e+05
24	.115e+01	.392e+05	.162e+05	.104e+04	.102e+05	.140e+05
25	.390e+00	.291e+05	.115e+05	.852e+03	.723e+04	.993e+04
26	.145e+01	.440e+05	.175e+05	.119e+04	.110e+05	.151e+05
27	.109e+01	.397e+05	.159e+05	.104e+04	.100e+05	.138e+05
28	.116e+01	.401e+05	.162e+05	.103e+04	.102e+05	.141e+05
29	.115e+01	.397e+05	.162e+05	.102e+04	.102e+05	.140e+05
30	.384e+00	.293e-05	.114e+05	.833e+03	.718e+04	.986e+04
31	.146e+01	.446e+05	.175e+05	.116e+04	.110e+05	.152e+05
32	.109e+01	.402e+05	.159e+05	.103e+04	.100e+05	.138e+05
33	.116e+01	.405e+05	.162e+05	.102e+04	.102e+05	.141e+05
34	.115e+01	.401e+05	.162e+05	.101e+04	.102e+05	.140e+05
35	.378e+00	.294e+05	.113e+05	.823e+03	.714e+04	.981e+04
36	.147e+01	.450e+05	.175e+05	.117e+04	.110e+05	.152e+05
37	.110e+01	.404e+05	.159e+05	.102e+04	.100e+05	.138e+05
38	.117e+01	.408e+05	.162e+05	.101e+04	.102e+05	.141e+05
39	.116e+01	.403e+05	.162e+05	.100e+04	.102e+05	.140e+05
40	.375e+00	.294e+05	.113e+05	.816e+03	.711e+04	.978e+04
41	.147e+01	.453e+05	.175e+05	.116e+04	.110e+05	.152e+05
42	.110e+01	.406e+05	.159e+05	.101e+04	.100e+05	.138e+05
43	.117e+01	.410e+05	.162e+05	.101e+04	.102e+05	.141e+05
44	.116e+01	.405e+05	.162e+05	.995e+03	.102e+05	.140e+05
45	.373e+00	.295e+05	.113e+05	.811e+03	.709e+04	.976e+04
46	.148e+01	.454e+05	.176e+05	.116e+04	.111e+05	.152e+05
47	.110e+01	.407e+05	.159e+05	.101e+04	.100e+05	.138e+05
48	.117e+01	.411e+05	.162e+05	.101e+04	.102e+05	.141e+05
49	.116e+01	.406e+05	.162e+05	.991e+03	.102e+05	.140e+05
50	.372e+00	.295e-05	.112e+05	.808e+03	.708e+04	.975e+04
51	.687e+00	.359e+05	.128e+05	.105e+04	.872e+04	.120e+05
52	.616e+00	.347e+05	.134e+05	.107e+04	.845e+04	.116e+05
53	.638e+00	.352e+05	.125e+05	.111e+04	.856e+04	.117e+05
54	.638e+00	.354e+05	.136e+05	.113e+04	.657e+04	.117e+05

55	.344e+00	.309e+05	.112e+05	.102e+04	.710e+04	.974e+04
56	.660e+00	.377e+05	.137e+05	.122e+04	.868e+04	.119e+05
57	.586e+00	.363e+05	.133e+05	.117e+04	.837e+04	.115e+05
58	.605e+00	.367e+05	.134e+05	.117e+04	.845e+04	.116e+05
59	.605e+00	.367e+05	.134e+05	.116e+04	.844e+04	.116e+05
60	.307e+00	.316e+05	.109e+05	.103e+04	.687e+04	.944e+04
61	.630e+00	.390e+05	.136e+05	.124e+04	.856e+04	.118e+05
62	.555e+00	.374e+05	.131e+05	.117e+04	.823e+04	.113e+05
63	.577e+00	.377e+05	.132e+05	.117e+04	.831e+04	.114e+05
64	.578e+00	.377e+05	.132e+05	.115e+04	.831e+04	.114e+05
65	.285e+00	.321e+05	.107e+05	.102e+04	.671e+04	.924e+04
66	.607e+00	.400e+05	.134e+05	.124e+04	.845e+04	.116e+05
67	.532e+00	.382e+05	.129e+05	.116e+04	.812e+04	.112e+05
68	.556e+00	.385e+05	.131e+05	.116e+04	.821e+04	.113e+05
69	.558e+00	.384e+05	.131e+05	.115e+04	.822e+04	.113e+05
70	.270e+00	.324e+05	.105e+05	.101e+04	.660e+04	.910e+04
71	.590e+00	.407e+05	.133e+05	.124e+04	.838e+04	.115e+05
72	.517e+00	.388e+05	.128e+05	.116e+04	.804e+04	.111e+05
73	.541e+00	.391e+05	.130e+05	.115e+04	.814e+04	.112e+05
74	.544e+00	.390e+05	.130e+05	.114e+04	.815e+04	.112e+05
75	.260e+00	.327e+05	.104e+05	.101e+04	.652e+04	.899e+04
76	.578e+00	.412e+05	.132e+05	.124e+04	.832e+04	.115e+05
77	.505e+00	.392e+05	.127e+05	.116e+04	.798e+04	.110e+05
78	.530e+00	.395e+05	.129e+05	.115e+04	.809e+04	.112e+05
79	.534e+00	.393e+05	.129e+05	.114e+04	.810e+04	.112e+05
80	.253e+00	.329e+05	.103e+05	.101e+04	.646e+04	.892e+04
81	.570e+00	.415e+05	.132e+05	.124e+04	.828e+04	.114e+05
82	.497e+00	.395e+05	.127e+05	.116e+04	.794e+04	.110e+05
83	.523e+00	.398e+05	.128e+05	.115e+04	.805e+04	.111e+05
84	.527e+00	.396e+05	.128e+05	.114e+04	.807e+04	.111e+05
85	.248e+00	.330e+05	.102e+05	.100e+04	.642e+04	.887e+04
86	.564e+00	.416e+05	.132e+05	.124e+04	.825e+04	.114e+05
87	.492e+00	.397e+05	.126e+05	.115e+04	.791e+04	.109e+05
88	.518e+00	.400e+05	.128e+05	.115e+04	.803e+04	.111e+05
89	.522e+00	.398e+05	.128e+05	.113e+04	.804e+04	.111e+05
90	.244e+00	.331e+05	.102e+05	.100e+04	.639e+04	.883e+04
91	.560e+00	.420e+05	.131e+05	.124e+04	.823e+04	.114e+05
92	.488e+00	.399e+05	.126e+05	.115e+04	.789e+04	.109e+05
93	.514e+00	.401e+05	.128e+05	.115e+04	.801e+04	.111e+05
94	.519e+00	.399e+05	.128e+05	.113e+04	.802e+04	.111e+05
95	.242e+00	.331e+05	.102e+05	.100e+04	.637e+04	.881e+04
96	.557e+00	.421e+05	.131e+05	.123e+04	.822e+04	.114e+05
97	.485e+00	.400e+05	.126e+05	.115e+04	.788e+04	.109e+05
98	.511e+00	.402e+05	.127e+05	.115e+04	.799e+04	.110e+05
99	.516e+00	.400e+05	.128e+05	.113e+04	.801e+04	.111e+05
100	.240e+00	.332e+05	.101e+05	.999e+03	.636e+04	.879e+04
101	.555e+00	.422e+05	.131e+05	.123e+04	.821e+04	.113e+05
102	.483e+00	.400e+05	.126e+05	.115e+04	.787e+04	.109e+05
103	.510e+00	.403e+05	.127e+05	.114e+04	.798e+04	.110e+05
104	.515e+00	.401e+05	.128e+05	.113e+04	.800e+04	.111e+05
105	.239e+00	.332e+05	.101e+05	.998e+03	.635e+04	.877e+04
106	.554e+00	.423e+05	.131e+05	.123e+04	.820e+04	.113e+05
107	.482e+00	.401e+05	.125e+05	.115e+04	.786e+04	.109e+05
108	.509e+00	.404e+05	.127e+05	.114e+04	.798e+04	.110e+05
109	.514e+00	.402e+05	.128e+05	.113e+04	.800e+04	.111e+05
110	.238e+00	.332e+05	.101e+05	.997e+03	.634e+04	.877e+04
111	.553e+00	.423e+05	.131e+05	.123e+04	.820e+04	.113e+05
112	.481e+00	.401e+05	.125e+05	.115e+04	.786e+04	.109e+05
113	.508e+00	.404e+05	.127e+05	.114e+04	.797e+04	.110e+05
114	.510e+00	.402e+05	.127e+05	.113e+04	.799e+04	.110e+05
115	.238e+00	.332e+05	.101e+05	.996e+03	.634e+04	.876e+04
116	.553e+00	.423e+05	.131e+05	.123e+04	.819e+04	.113e+05
117	.481e+00	.402e+05	.125e+05	.115e+04	.786e+04	.109e+05
118	.507e+00	.404e+05	.127e+05	.114e+04	.797e+04	.110e+05

119	.513e+00	.402e+05	.127e+05	.113e+04	.799e+04	.110e+05
120	.238e+00	.333e+05	.101e+05	.995e+03	.633e+04	.876e+04
121	.552e+00	.424e+05	.131e+05	.123e+04	.819e+04	.113e+05
122	.481e+00	.402e+05	.125e+05	.115e+04	.785e+04	.109e+05
123	.507e+00	.404e+05	.127e+05	.114e+04	.797e+04	.110e+05
124	.512e+00	.402e+05	.127e+05	.113e+04	.799e+04	.110e+05
125	.237e+00	.333e+05	.101e+05	.995e+03	.633e+04	.875e+04
126	.552e+00	.424e+05	.131e+05	.123e+04	.819e+04	.113e+05
127	.481e+00	.402e+05	.125e+05	.115e+04	.785e+04	.109e+05
128	.507e+00	.404e+05	.127e+05	.114e+04	.797e+04	.110e+05
129	.512e+00	.402e+05	.127e+05	.113e+04	.799e+04	.110e+05
130	.237e+00	.333e+05	.101e+05	.994e+03	.633e+04	.875e+04
131	.552e+00	.424e+05	.131e+05	.123e+04	.819e+04	.113e+05
132	.481e+00	.402e+05	.125e+05	.115e+04	.785e+04	.109e+05
133	.507e+00	.405e+05	.127e+05	.114e+04	.797e+04	.110e+05
134	.512e+00	.403e+05	.127e+05	.113e+04	.799e+04	.110e+05
135	.237e+00	.333e+05	.101e+05	.994e+03	.633e+04	.875e+04
136	.552e+00	.424e+05	.131e+05	.123e+04	.819e+04	.113e+05
137	.481e+00	.402e+05	.125e+05	.115e+04	.785e+04	.109e+05
138	.507e+00	.405e+05	.127e+05	.114e+04	.797e+04	.110e+05
139	.512e+00	.403e+05	.127e+05	.112e+04	.799e+04	.110e+05
140	.237e+00	.333e+05	.101e+05	.993e+03	.633e+04	.875e+04
141	.251e+00	.351e+05	.104e+05	.111e+04	.654e+04	.903e+04
142	.226e+00	.349e+05	.102e+05	.115e+04	.639e+04	.881e+04
143	.214e+00	.352e+05	.101e+05	.121e+04	.633e+04	.873e+04
144	.202e+00	.353e+05	.997e+04	.125e+04	.627e+04	.864e+04
145	.182e+00	.358e+05	.974e+04	.128e+04	.613e+04	.844e+04
146	.176e+00	.358e+05	.968e+04	.132e+04	.609e+04	.839e+04
147	.170e+00	.359e+05	.963e+04	.135e+04	.607e+04	.835e+04
148	.165e+00	.359e+05	.959e+04	.138e+04	.604e+04	.831e+04
149	.161e+00	.360e+05	.954e+04	.140e+04	.602e+04	.827e+04
150	.148e+00	.365e+05	.937e+04	.142e+04	.591e+04	.812e+04
151	.145e+00	.364e+05	.934e+04	.144e+04	.589e+04	.809e+04
152	.144e+00	.364e+05	.934e+04	.146e+04	.589e+04	.809e+04
153	.142e+00	.364e+05	.932e+04	.148e+04	.589e+04	.806e+04
154	.140e+00	.364e+05	.931e+04	.149e+04	.588e+04	.807e+04
155	.131e+00	.369e+05	.917e+04	.150e+04	.579e+04	.795e+04
156	.130e+00	.367e+05	.915e+04	.152e+04	.578e+04	.793e+04
157	.130e+00	.367e+05	.917e+04	.153e+04	.580e+04	.794e+04
158	.129e+00	.367e+05	.917e+04	.154e+04	.580e+04	.795e+04
159	.129e+00	.367e+05	.917e+04	.155e+04	.580e+04	.795e+04
160	.121e+00	.371e+05	.904e+04	.156e+04	.572e+04	.783e+04
161	.121e+00	.369e+05	.903e+04	.157e+04	.572e+04	.783e+04
162	.121e+00	.369e+05	.906e+04	.158e+04	.573e+04	.785e+04
163	.122e+00	.369e+05	.907e+04	.158e+04	.574e+04	.786e+04
164	.122e+00	.369e+05	.907e+04	.158e+04	.575e+04	.786e+04
165	.114e+00	.373e+05	.894e+04	.159e+04	.566e+04	.775e+04
166	.115e+00	.371e+05	.896e+04	.160e+04	.568e+04	.776e+04
167	.116e+00	.371e+05	.898e+04	.161e+04	.569e+04	.779e+04
168	.117e+00	.371e+05	.900e+04	.161e+04	.570e+04	.780e+04
169	.117e+00	.371e+05	.901e+04	.161e+04	.571e+04	.781e+04
170	.110e+00	.374e+05	.887e+04	.162e+04	.562e+04	.769e+04
171	.111e+00	.373e+05	.890e+04	.162e+04	.565e+04	.772e+04
172	.112e+00	.373e+05	.893e+04	.163e+04	.566e+04	.774e+04
173	.113e+00	.373e+05	.895e+04	.163e+04	.567e+04	.775e+04
174	.113e+00	.373e+05	.896e+04	.163e+04	.568e+04	.776e+04
175	.106e+00	.375e+05	.892e+04	.163e+04	.559e+04	.764e+04
176	.108e+00	.375e+05	.888e+04	.164e+04	.562e+04	.768e+04
177	.109e+00	.375e+05	.889e+04	.164e+04	.564e+04	.770e+04
178	.110e+00	.375e+05	.890e+04	.164e+04	.565e+04	.772e+04
179	.111e+00	.375e+05	.892e+04	.164e+04	.566e+04	.773e+04
180	.103e+00	.376e+05	.877e+04	.165e+04	.556e+04	.760e+04
181	.101e+00	.378e+05	.873e+04	.166e+04	.554e+04	.757e+04
182	.982e-01	.378e+05	.868e+04	.167e+04	.551e+04	.753e+04

RD-A172 786

A METHOD FOR DETERMINING THE HIGH ENERGY PHOTON
SPECTRUM OF A PULSED PLASMA SOURCE(U) AIR FORCE INST OF
TECH WRIGHT-PATTERSON AFB OH SCHOOL OF ENGI.

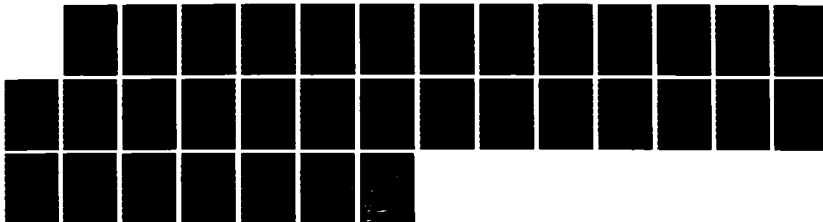
2/2

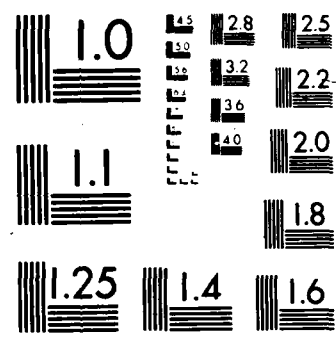
UNCLASSIFIED

C W BEERSON MAR 84 AFIT/GNE/PH/84M-1

F/G 18/4

NL





183	.960e-01	.379e+05	.865e+04	.169e+04	.549e+04	.749e+04
184	.940e-01	.380e+05	.861e+04	.170e+04	.547e+04	.746e+04
185	.902e-01	.381e+05	.854e+04	.172e+04	.543e+04	.740e+04
186	.891e-01	.381e+05	.853e+04	.173e+04	.542e+04	.739e+04
187	.879e-01	.381e+05	.851e+04	.175e+04	.542e+04	.737e+04
188	.869e-01	.382e+05	.849e+04	.176e+04	.541e+04	.736e+04
189	.860e-01	.382e+05	.848e+04	.177e+04	.540e+04	.735e+04
190	.833e-01	.383e+05	.842e+04	.178e+04	.537e+04	.730e+04
191	.828e-01	.383e+05	.842e+04	.180e+04	.537e+04	.729e+04
192	.823e-01	.383e+05	.841e+04	.181e+04	.537e+04	.729e+04
193	.818e-01	.383e+05	.841e+04	.182e+04	.536e+04	.728e+04
194	.814e-01	.383e+05	.840e+04	.182e+04	.536e+04	.728e+04
195	.792e-01	.384e+05	.835e+04	.183e+04	.533e+04	.724e+04
196	.790e-01	.384e+05	.835e+04	.184e+04	.533e+04	.724e+04
197	.789e-01	.384e+05	.835e+04	.185e+04	.534e+04	.724e+04
198	.787e-01	.384e+05	.835e+04	.186e+04	.534e+04	.724e+04
199	.785e-01	.384e+05	.835e+04	.186e+04	.534e+04	.723e+04
200	.766e-01	.385e+05	.830e+04	.187e+04	.531e+04	.719e+04
201	.766e-01	.384e+05	.831e+04	.188e+04	.531e+04	.720e+04
202	.767e-01	.384e+05	.831e+04	.188e+04	.532e+04	.720e+04
203	.767e-01	.384e+05	.831e+04	.189e+04	.532e+04	.720e+04
204	.766e-01	.384e+05	.831e+04	.189e+04	.532e+04	.720e+04
205	.749e-01	.385e+05	.827e+04	.189e+04	.529e+04	.717e+04
206	.751e-01	.385e+05	.827e+04	.190e+04	.530e+04	.717e+04
207	.752e-01	.385e+05	.828e+04	.190e+04	.530e+04	.718e+04
208	.753e-01	.385e+05	.828e+04	.191e+04	.531e+04	.718e+04
209	.754e-01	.385e+05	.829e+04	.191e+04	.531e+04	.718e+04
210	.738e-01	.386e+05	.824e+04	.191e+04	.528e+04	.714e+04
211	.740e-01	.386e+05	.825e+04	.192e+04	.529e+04	.715e+04
212	.742e-01	.385e+05	.826e+04	.192e+04	.529e+04	.716e+04
213	.744e-01	.385e+05	.826e+04	.192e+04	.530e+04	.716e+04
214	.745e-01	.385e+05	.827e+04	.192e+04	.530e+04	.716e+04
215	.729e-01	.386e+05	.822e+04	.192e+04	.527e+04	.713e+04
216	.733e-01	.386e+05	.824e+04	.193e+04	.528e+04	.714e+04
217	.735e-01	.385e+05	.824e+04	.193e+04	.529e+04	.714e+04
218	.737e-01	.385e+05	.825e+04	.193e+04	.529e+04	.715e+04
219	.738e-01	.385e+05	.825e+04	.193e+04	.529e+04	.715e+04
220	.723e-01	.386e+05	.821e+04	.193e+04	.527e+04	.712e+04
221	.727e-01	.386e+05	.822e+04	.194e+04	.528e+04	.713e+04
222	.730e-01	.386e+05	.823e+04	.194e+04	.528e+04	.713e+04
223	.732e-01	.386e+05	.824e+04	.194e+04	.528e+04	.714e+04
224	.733e-01	.385e+05	.824e+04	.194e+04	.529e+04	.714e+04
225	.718e-01	.386e+05	.820e+04	.194e+04	.526e+04	.711e+04
226	.723e-01	.386e+05	.822e+04	.194e+04	.527e+04	.712e+04
227	.725e-01	.386e+05	.822e+04	.195e+04	.528e+04	.713e+04
228	.728e-01	.386e+05	.823e+04	.194e+04	.528e+04	.713e+04
229	.729e-01	.386e+05	.823e+04	.194e+04	.528e+04	.714e+04
230	.714e-01	.386e+05	.819e+04	.195e+04	.526e+04	.710e+04
231	.720e-01	.386e+05	.821e+04	.195e+04	.527e+04	.711e+04
232	.722e-01	.386e+05	.821e+04	.195e+04	.527e+04	.712e+04
233	.725e-01	.386e+05	.822e+04	.195e+04	.528e+04	.713e+04
234	.726e-01	.386e+05	.823e+04	.195e+04	.528e+04	.713e+04
235	.711e-01	.386e+05	.818e+04	.195e+04	.525e+04	.709e+04
236	.717e-01	.307e-05	.820e+04	.195e+04	.527e+04	.711e+04
237	.720e-01	.386e+05	.821e+04	.195e+04	.527e+04	.711e+04
238	.723e-01	.386e+05	.822e+04	.195e+04	.527e+04	.712e+04
239	.724e-01	.386e+05	.822e+04	.195e+04	.528e+04	.712e+04
240	.708e-01	.386e+05	.818e+04	.195e+04	.525e+04	.709e+04
241	.715e-01	.387e-05	.820e+04	.196e+04	.526e+04	.710e+04
242	.717e-01	.386e+05	.820e+04	.196e+04	.527e+04	.711e+04
243	.720e-01	.386e+05	.821e+04	.196e+04	.527e+04	.712e+04
244	.722e-01	.386e+05	.822e+04	.195e+04	.528e+04	.712e+04
245	.706e-01	.387e+05	.817e+04	.196e+04	.525e+04	.708e+04
246	.713e-01	.387e+05	.819e+04	.196e+04	.526e+04	.710e+04

247	.715e-01	.387e+05	.820e+04	.196e+04	.527e+04	.711e+04
248	.718e-01	.387e+05	.821e+04	.196e+04	.527e+04	.711e+04
249	.720e-01	.387e+05	.821e+04	.196e+04	.527e+04	.712e+04
250	.704e-01	.387e+05	.816e+04	.196e+04	.524e+04	.708e+04
251	.712e-01	.387e+05	.819e+04	.196e+04	.526e+04	.710e+04
252	.714e-01	.387e+05	.819e+04	.196e+04	.526e+04	.710e+04
253	.716e-01	.387e+05	.820e+04	.196e+04	.527e+04	.711e+04
254	.718e-01	.387e+05	.821e+04	.196e+04	.527e+04	.711e+04
255	.702e-01	.387e+05	.816e+04	.196e+04	.524e+04	.707e+04
256	.710e-01	.387e+05	.819e+04	.197e+04	.526e+04	.710e+04
257	.712e-01	.387e+05	.819e+04	.196e+04	.526e+04	.710e+04
258	.715e-01	.387e+05	.820e+04	.196e+04	.527e+04	.710e+04
259	.716e-01	.387e+05	.820e+04	.196e+04	.527e+04	.711e+04
260	.700e-01	.387e+05	.815e+04	.196e+04	.524e+04	.707e+04
261	.709e-01	.387e+05	.818e+04	.197e+04	.526e+04	.709e+04
262	.711e-01	.387e+05	.819e+04	.197e+04	.526e+04	.710e+04
263	.713e-01	.387e+05	.819e+04	.196e+04	.527e+04	.710e+04
264	.715e-01	.387e+05	.820e+04	.196e+04	.527e+04	.711e+04
265	.698e-01	.387e+05	.815e+04	.196e+04	.524e+04	.706e+04
266	.708e-01	.388e+05	.818e+04	.197e+04	.526e+04	.709e+04
267	.709e-01	.387e+05	.818e+04	.197e+04	.526e+04	.709e+04
268	.712e-01	.387e+05	.819e+04	.197e+04	.526e+04	.710e+04
269	.714e-01	.387e+05	.820e+04	.196e+04	.527e+04	.710e+04
270	.697e-01	.387e+05	.815e+04	.196e+04	.523e+04	.706e+04
271	.707e-01	.388e+05	.818e+04	.197e+04	.526e+04	.709e+04
272	.708e-01	.387e+05	.818e+04	.197e+04	.526e+04	.709e+04
273	.711e-01	.387e+05	.819e+04	.197e+04	.526e+04	.710e+04
274	.712e-01	.387e+05	.819e+04	.197e+04	.526e+04	.710e+04
275	.695e-01	.387e+05	.814e+04	.197e+04	.523e+04	.706e+04
276	.706e-01	.388e+05	.818e+04	.197e+04	.526e+04	.709e+04
277	.707e-01	.388e+05	.818e+04	.197e+04	.526e+04	.709e+04
278	.710e-01	.388e+05	.819e+04	.197e+04	.526e+04	.709e+04
279	.711e-01	.387e+05	.819e+04	.197e+04	.526e+04	.710e+04
280	.694e-01	.387e+05	.814e+04	.197e+04	.523e+04	.705e+04
281	.705e-01	.388e+05	.817e+04	.197e+04	.525e+04	.708e+04
282	.706e-01	.388e+05	.818e+04	.197e+04	.526e+04	.709e+04
283	.708e-01	.388e+05	.816e+04	.197e+04	.526e+04	.709e+04
284	.710e-01	.388e+05	.819e+04	.197e+04	.526e+04	.710e+04
285	.692e-01	.387e+05	.813e+04	.197e+04	.523e+04	.705e+04
286	.704e-01	.388e+05	.817e+04	.196e+04	.525e+04	.708e+04
287	.705e-01	.388e+05	.817e+04	.197e+04	.525e+04	.708e+04
288	.707e-01	.388e+05	.818e+04	.197e+04	.526e+04	.709e+04
289	.709e-01	.388e+05	.818e+04	.197e+04	.526e+04	.709e+04
290	.691e-01	.387e+05	.813e+04	.197e+04	.523e+04	.705e+04
291	.703e-01	.388e+05	.817e+04	.198e+04	.525e+04	.706e+04
292	.704e-01	.388e+05	.817e+04	.197e+04	.525e+04	.708e+04
293	.706e-01	.388e+05	.818e+04	.197e+04	.526e+04	.709e+04
294	.708e-01	.388e+05	.818e+04	.197e+04	.526e+04	.709e+04
295	.690e-01	.387e+05	.813e+04	.197e+04	.523e+04	.704e+04
296	.703e-01	.389e+05	.817e+04	.198e+04	.525e+04	.708e+04
297	.703e-01	.388e+05	.817e+04	.198e+04	.525e+04	.708e+04
298	.705e-01	.388e+05	.818e+04	.197e+04	.526e+04	.709e+04
299	.707e-01	.388e+05	.818e+04	.197e+04	.526e+04	.709e+04
300	.668e-01	.387e+05	.812e+04	.197e+04	.522e+04	.704e+04
301	.702e-01	.389e+05	.817e+04	.196e+04	.525e+04	.708e+04
302	.702e-01	.388e+05	.817e+04	.198e+04	.525e+04	.708e+04
303	.704e-01	.388e+05	.817e+04	.198e+04	.525e+04	.708e+04
304	.706e-01	.388e+05	.818e+04	.197e+04	.526e+04	.709e+04
305	.607e-01	.387e+05	.812e+04	.197e+04	.522e+04	.704e+04
306	.701e-01	.389e+05	.816e+04	.196e+04	.525e+04	.708e+04
307	.701e-01	.388e+05	.816e+04	.196e+04	.525e+04	.708e+04
308	.704e-01	.388e+05	.817e+04	.198e+04	.525e+04	.708e+04
309	.705e-01	.388e+05	.818e+04	.198e+04	.526e+04	.708e+04
310	.686e-01	.387e+05	.812e+04	.197e+04	.522e+04	.703e+04

311	.700e-01	.389e+05	.816e+04	.198e+04	.525e+04	.707e+04
312	.700e-01	.388e+05	.816e+04	.198e+04	.525e+04	.707e+04
313	.703e-01	.388e+05	.817e+04	.198e+04	.525e+04	.708e+04
314	.704e-01	.388e+05	.817e+04	.198e+04	.525e+04	.708e+04
315	.685e-01	.387e+05	.811e+04	.198e+04	.522e+04	.703e+04
316	.700e-01	.389e+05	.816e+04	.198e+04	.525e+04	.707e+04
317	.700e-01	.389e+05	.816e+04	.198e+04	.525e+04	.707e+04
318	.702e-01	.389e+05	.817e+04	.198e+04	.525e+04	.708e+04
319	.703e-01	.389e+05	.817e+04	.198e+04	.525e+04	.708e+04
320	.684e-01	.387e+05	.811e+04	.198e+04	.522e+04	.703e+04
321	.699e-01	.389e+05	.816e+04	.199e+04	.525e+04	.707e+04
322	.699e-01	.389e+05	.816e+04	.198e+04	.525e+04	.707e+04
323	.701e-01	.389e+05	.816e+04	.198e+04	.525e+04	.708e+04
324	.703e-01	.389e+05	.817e+04	.198e+04	.525e+04	.708e+04
325	.683e-01	.387e+05	.811e+04	.198e+04	.522e+04	.703e+04
326	.698e-01	.389e+05	.816e+04	.199e+04	.525e+04	.707e+04
327	.698e-01	.389e+05	.816e+04	.198e+04	.525e+04	.707e+04
328	.700e-01	.389e+05	.816e+04	.198e+04	.525e+04	.707e+04
329	.702e-01	.389e+05	.817e+04	.198e+04	.525e+04	.708e+04
330	.682e-01	.388e+05	.811e+04	.198e+04	.521e+04	.702e+04
331	.698e-01	.389e+05	.816e+04	.199e+04	.525e+04	.707e+04
332	.697e-01	.389e+05	.815e+04	.198e+04	.525e+04	.707e+04
333	.700e-01	.389e+05	.816e+04	.198e+04	.525e+04	.707e+04
334	.701e-01	.389e+05	.816e+04	.198e+04	.525e+04	.708e+04
335	.681e-01	.388e+05	.810e+04	.198e+04	.521e+04	.702e+04
336	.697e-01	.390e+05	.816e+04	.199e+04	.525e+04	.707e+04
337	.697e-01	.389e+05	.815e+04	.199e+04	.524e+04	.707e+04
338	.699e-01	.389e+05	.816e+04	.198e+04	.525e+04	.707e+04
339	.700e-01	.389e+05	.816e+04	.198e+04	.525e+04	.707e+04
340	.680e-01	.388e+05	.810e+04	.198e+04	.521e+04	.702e+04
341	.697e-01	.390e+05	.815e+04	.199e+04	.525e+04	.707e+04
342	.696e-01	.389e+05	.815e+04	.199e+04	.524e+04	.706e+04
343	.698e-01	.389e+05	.816e+04	.198e+04	.525e+04	.707e+04
344	.700e-01	.389e+05	.816e+04	.198e+04	.525e+04	.707e+04
345	.679e-01	.368e+05	.810e+04	.198e+04	.521e+04	.702e+04
346	.696e-01	.390e+05	.815e+04	.199e+04	.525e+04	.707e+04
347	.695e-01	.389e+05	.815e+04	.199e+04	.524e+04	.706e+04
348	.698e-01	.389e+05	.816e+04	.199e+04	.525e+04	.707e+04
349	.699e-01	.389e+05	.816e+04	.198e+04	.525e+04	.707e+04
350	.678e-01	.388e+05	.810e+04	.198e+04	.521e+04	.702e+04
351	.695e-01	.390e+05	.815e+04	.199e+04	.525e+04	.706e+04
352	.695e-01	.389e+05	.815e+04	.199e+04	.524e+04	.706e+04
353	.697e-01	.389e+05	.815e+04	.199e+04	.525e+04	.707e+04
354	.698e-01	.389e+05	.816e+04	.198e+04	.525e+04	.707e+04
355	.677e-01	.386e+05	.809e+04	.196e+04	.521e+04	.701e+04
356	.695e-01	.390e+05	.815e+04	.199e+04	.524e+04	.706e+04
357	.694e-01	.389e+05	.815e+04	.199e+04	.524e+04	.706e+04
358	.696e-01	.389e+05	.815e+04	.199e+04	.525e+04	.707e+04
359	.698e-01	.389e+05	.816e+04	.199e+04	.525e+04	.707e+04
360	.677e-01	.368e+05	.809e+04	.196e+04	.521e+04	.701e+04
361	.694e-01	.390e+05	.815e+04	.199e+04	.524e+04	.706e+04
362	.693e-01	.389e+05	.814e+04	.199e+04	.524e+04	.706e+04
363	.696e-01	.389e+05	.815e+04	.199e+04	.524e+04	.706e+04
364	.697e-01	.389e+05	.815e+04	.199e+04	.525e+04	.707e+04
365	.676e-01	.388e+05	.809e+04	.196e+04	.521e+04	.701e+04
366	.694e-01	.390e+05	.815e+04	.200e+04	.524e+04	.706e+04
367	.693e-01	.390e+05	.814e+04	.199e+04	.524e+04	.706e+04
368	.695e-01	.390e+05	.815e+04	.199e+04	.524e+04	.706e+04
369	.696e-01	.390e+05	.815e+04	.199e+04	.525e+04	.707e+04
370	.675e-01	.388e+05	.809e+04	.196e+04	.520e+04	.701e+04
371	.694e-01	.390e+05	.815e+04	.200e+04	.524e+04	.706e+04
372	.692e-01	.390e+05	.814e+04	.199e+04	.524e+04	.706e+04
373	.694e-01	.390e+05	.815e+04	.199e+04	.524e+04	.706e+04
374	.696e-01	.390e+05	.815e+04	.199e+04	.524e+04	.706e+04

951	.679e-01	.393e+05	.811e+04	.204e+04	.523e+04	.703e+04
952	.674e-01	.392e+05	.809e+04	.203e+04	.521e+04	.701e+04
953	.676e-01	.393e+05	.810e+04	.203e+04	.522e+04	.702e+04
954	.676e-01	.393e+05	.810e+04	.203e+04	.522e+04	.702e+04
955	.649e-01	.389e+05	.801e+04	.202e+04	.516e+04	.694e+04
956	.679e-01	.393e+05	.811e+04	.204e+04	.523e+04	.703e+04
957	.674e-01	.392e+05	.809e+04	.203e+04	.521e+04	.701e+04
958	.676e-01	.393e+05	.810e+04	.203e+04	.522e+04	.702e+04
959	.676e-01	.393e+05	.810e+04	.203e+04	.522e+04	.702e+04
960	.649e-01	.389e+05	.801e+04	.202e+04	.516e+04	.694e+04
961	.679e-01	.393e+05	.811e+04	.204e+04	.523e+04	.703e+04
962	.674e-01	.392e+05	.809e+04	.203e+04	.521e+04	.701e+04
963	.676e-01	.393e+05	.810e+04	.203e+04	.522e+04	.702e+04
964	.676e-01	.393e+05	.810e+04	.203e+04	.522e+04	.702e+04
965	.649e-01	.389e+05	.801e+04	.202e+04	.516e+04	.694e+04
966	.679e-01	.393e+05	.811e+04	.204e+04	.523e+04	.703e+04
967	.673e-01	.392e+05	.809e+04	.203e+04	.521e+04	.701e+04
968	.676e-01	.393e+05	.810e+04	.203e+04	.522e+04	.702e+04
969	.676e-01	.393e+05	.810e+04	.203e+04	.522e+04	.702e+04
970	.649e-01	.389e+05	.801e+04	.202e+04	.516e+04	.694e+04
971	.679e-01	.393e+05	.811e+04	.204e+04	.523e+04	.703e+04
972	.673e-01	.392e+05	.809e+04	.203e+04	.521e+04	.701e+04
973	.676e-01	.393e+05	.810e+04	.203e+04	.522e+04	.702e+04
974	.676e-01	.393e+05	.810e+04	.203e+04	.522e+04	.702e+04
975	.649e-01	.389e+05	.801e+04	.202e+04	.516e+04	.694e+04
976	.679e-01	.393e+05	.811e+04	.204e+04	.523e+04	.703e+04
977	.673e-01	.392e+05	.809e+04	.203e+04	.521e+04	.701e+04
978	.676e-01	.393e+05	.810e+04	.203e+04	.522e+04	.702e+04
979	.676e-01	.393e+05	.810e+04	.203e+04	.522e+04	.702e+04
980	.649e-01	.389e+05	.801e+04	.202e+04	.516e+04	.694e+04
981	.679e-01	.393e+05	.811e+04	.204e+04	.523e+04	.703e+04
982	.673e-01	.392e+05	.809e+04	.203e+04	.521e+04	.701e+04
983	.676e-01	.393e+05	.810e+04	.203e+04	.522e+04	.702e+04
984	.676e-01	.393e+05	.810e+04	.203e+04	.522e+04	.702e+04
985	.649e-01	.389e+05	.801e+04	.202e+04	.516e+04	.694e+04
986	.678e-01	.393e+05	.811e+04	.204e+04	.523e+04	.703e+04
987	.673e-01	.392e+05	.809e+04	.203e+04	.521e+04	.701e+04
988	.676e-01	.393e+05	.810e+04	.203e+04	.522e+04	.702e+04
989	.676e-01	.393e+05	.810e+04	.203e+04	.522e+04	.702e+04
990	.649e-01	.389e+05	.801e+04	.202e+04	.516e+04	.694e+04
991	.678e-01	.393e+05	.811e+04	.204e+04	.523e+04	.703e+04
992	.673e-01	.392e+05	.809e+04	.203e+04	.521e+04	.701e+04
993	.675e-01	.393e+05	.810e+04	.203e+04	.522e+04	.702e+04
994	.676e-01	.393e+05	.810e+04	.203e+04	.522e+04	.702e+04
995	.649e-01	.389e+05	.801e+04	.202e+04	.516e+04	.694e+04
996	.676e-01	.393e+05	.811e+04	.204e+04	.523e+04	.703e+04
997	.673e-01	.392e+05	.809e+04	.203e+04	.521e+04	.701e+04
998	.675e-01	.393e+05	.810e+04	.203e+04	.522e+04	.702e+04
999	.648e-01	.389e+05	.801e+04	.202e+04	.516e+04	.694e+04
1000	.649e-01	.390e+05	.801e+04	.204e+04	.517e+04	.694e+04

DET ODS. SIGNAL CALC. SIGNAL

1	.3920e+05	.3896e+05
2	.5300e+04	.8813e+04
3	.1220e+04	.2038e+04
4	.6688e+04	.5169e+04
5	.6899e+04	.6945e+04

EE(J) (Fe) SPEC(J) (Watts/kJ) TSPEC(J) (Watts)

35.8888	.2546e+09	.3564e+09
36.4888	.9718e+08	.4978e+09
37.8568	.4885e+08	.5717e+09
39.3782	.2458e+08	.6105e+09
48.9458	.1237e+08	.6307e+09
42.5828	.6221e+07	.6413e+09
44.2862	.3129e+07	.6468e+09
46.0576	.1574e+07	.6497e+09
47.8999	.7916e+06	.6513e+09
49.8159	.3981e+06	.6521e+09
51.8085	.2001e+06	.6525e+09
53.8809	.1007e+06	.6527e+09
56.0361	.5068e+05	.6528e+09
58.2775	.2549e+05	.6529e+09
60.6086	.1290e+05	.6529e+09
63.0330	.6523e+04	.6529e+09
65.5543	.3298e+04	.6529e+09
68.1765	.1698e+04	.6529e+09
70.9035	.8745e+03	.6529e+09
73.7397	.4503e+03	.6529e+09
76.6892	.2400e+03	.6529e+09
79.7568	.1280e+03	.6529e+09
82.9471	.6826e+02	.6529e+09
86.2650	.3818e+02	.6529e+09
89.7156	.2132e+02	.6529e+09
93.3042	.1193e+02	.6529e+09
97.0363	.7075e+01	.6529e+09
100.9178	.4197e+01	.6529e+09
104.9545	.2498e+01	.6529e+09
109.1527	.1572e+01	.6529e+09
113.5188	.9925e+00	.6529e+09
118.0595	.6267e+00	.6529e+09
122.7819	.4214e+00	.6529e+09
127.6932	.2834e+00	.6529e+09
132.8009	.1906e+00	.6529e+09
136.1129	.1364e+00	.6529e+09
143.6374	.9755e-01	.6529e+09
149.3829	.6980e-01	.6529e+09
155.3582	.5296e-01	.6529e+09
161.5725	.4018e-01	.6529e+09
168.0354	.3049e-01	.6529e+09
174.7568	.2443e-01	.6529e+09
181.7471	.1958e-01	.6529e+09
189.0170	.1569e-01	.6529e+09
196.5776	.1321e-01	.6529e+09
204.4407	.1112e-01	.6529e+09
212.6184	.9365e-02	.6529e+09
221.1231	.8239e-02	.6529e+09
229.9680	.7249e-02	.6529e+09
239.1667	.6378e-02	.6529e+09
248.7334	.5833e-02	.6529e+09
258.6827	.5334e-02	.6529e+09
269.0300	.4878e-02	.6529e+09
279.7912	.4613e-02	.6529e+09
290.9828	.4363e-02	.6529e+09
302.6222	.4127e-02	.6529e+09
314.7271	.4018e-02	.6529e+09
327.3161	.3912e-02	.6529e+09
340.4088	.3809e-02	.6529e+09
354.0251	.3803e-02	.6529e+09
368.1861	.3798e-02	.6529e+09
362.9135	.3792e-02	.6529e+09
398.2300	.3866e-02	.6529e+09
414.1592	.3994e-02	.6529e+09

430.7256	.4099e-02	.6529e+09
447.9546	.4127e-02	.6529e+09
465.8727	.4149e-02	.6529e+09
484.5076	.4167e-02	.6529e+09
503.8879	.4072e-02	.6529e+09
524.0434	.3977e-02	.6529e+09
545.0051	.3880e-02	.6529e+09
566.8053	.3693e-02	.6529e+09
589.4775	.3496e-02	.6529e+09
613.0566	.3313e-02	.6529e+09
637.5788	.3183e-02	.6529e+09
663.0619	.3058e-02	.6529e+09
689.6052	.2938e-02	.6529e+09
717.1893	.2849e-02	.6529e+09
745.8769	.2763e-02	.6529e+09
775.7119	.2680e-02	.6529e+09
806.7404	.2618e-02	.6529e+09
839.0099	.2558e-02	.6529e+09
872.5703	.2500e-02	.6529e+09
907.4731	.2457e-02	.6529e+09
943.7720	.2415e-02	.6529e+09
981.5228	.2374e-02	.6529e+09
1020.7837	.2345e-02	.6529e+09
1061.6150	.2315e-02	.6529e+09
1104.0796	.2286e-02	.6529e+09
1148.2427	.2265e-02	.6529e+09
1194.1724	.2245e-02	.6529e+09
1241.9392	.2224e-02	.6529e+09
1291.6167	.2209e-02	.6529e+09
1343.2814	.2193e-02	.6529e+09
1397.0126	.2178e-02	.6529e+09
1452.0931	.2166e-02	.6529e+09
1511.0068	.2154e-02	.6529e+09
1571.4491	.2142e-02	.6529e+09
1634.3070	.2130e-02	.6529e+09
1699.6792	.2118e-02	.6529e+09

*** COMPLETION OF COMPUTATION ***

***** IFLAG= 708

APPENDIX D

APPENDIX D

Listing of Program PIN

This is a listing of the pre-processor program PIN. As listed, this program will execute on a VAX 11/780 under the UNIX operating system. By changing the OPEN statements in subroutines DATIN and DATOUT, the program will run under the VMS operating system.


```

      WRITE(6,16) J , I
      READ(2,15) MATNUM(I,J)
      WRITE(6,17) J , I
      READ(2,18) DEL(I,J)
      FORMAT(I1)
15      FORMAT(' Enter material number of filter ',I2,
16      1 ' of detector',I2)
17      FORMAT(' Enter thickness in cm of filter ',I2,
18      1 ' of detector',I2)
18      FORMAT(E16.8)
20      CONTINUE
100     CONTINUE
C
C      Input initial spectrum, iteration/convergence parameters
C
      WRITE(6,200)
200     FORMAT(' Flat/Two-Temperature exponential spectrum? (1/0)',*
1   '(This is for DCON)')
      READ(2,201) IS
201     FORMAT(I1)
      SO = -1.0
      IF ( IS .EQ. 0 ) GOTO 210
      WRITE(6,202)
202     FORMAT(' Enter initial flat spectrum value:')
      READ(2,203) SO
203     FORMAT(E16.8)
      GOTO 220
210     CONTINUE
C
C      Two-Temp spectrum of the form:
C      Initial spectrum = AA * DEXP( T1 / ENERGY ) +
C                           BB * DEXP( T2 / ENERGY )
C      is to be used as the initial spectrum for DCON
C
      WRITE(6,211)
211     FORMAT(' Enter T1')
      READ(2,203) T1
      WRITE(6,212)
212     FORMAT(' Enter T2')
      READ(2,203) T2
      WRITE(6,213)
213     FORMAT(' Enter AA')
      READ(2,203) AA
      WRITE(6,214)
214     FORMAT(' Enter BB')
      READ(2,203) BB
220     CONTINUE
      WRITE(6,230)
230     FORMAT(' Smoothing? (1/0)')
      READ(2,201) NP
      WRITE(6,240)
240     FORMAT(' Enter max error ERMAX')
      READ(2,203) ERMAX
      WRITE(6,250)
250     FORMAT(' Enter max. iterations KITMAX (9999 MAX)')
      READ(2,251) KITMAX
251     FORMAT(I4)
      WRITE(6,260)
260     FORMAT(' New trial spectrum or previous spectrum? (1/0)')
      READ(2,201) NSPEC
C
      WRITE(6,270)
270     FORMAT(' Enter number of energy groups to be used (100 max)')

```

```
READ(2,251) NE
WRITE(6,288)
288 FORMAT(' Enter lower limit of the energy groups')
READ(2,283) E1
WRITE(6,298)
298 FORMAT(' Enter energy group ratio')
READ(2,293) RATIO
CLOSE(UNIT=2)
RETURN
END
```

```

SUBROUTINE DATGEN
COMMON / ALL / NDET , KITMAX , E1 , RATIO ,
1 NFILT(15) , MATEUM(15,15) , VO(15,281) , TRES(288) ,
2 DEL(15,15) , SO , ISHOT ,
3 NSPEC , T1 , T2 , T3 , T4 , CC , DD ,
4 AA , BB , ND , NE , NP ,
5 KITP , ERROR , ERMAX

C
C Get detector area in square cm...
C
PI = 4.0 * ATAN(1.0)
DETA = PI * ( 2.54 * 1.125 ) ** 2
C
C Generate detector responses in amps*4PI OMEGA*(1/50.)...
C
DO 1 I = 1 , NDET
C
C Vacuum chamber radius in cm...
C
R = 14.2875
DO 10 J = 1 , NFILT(I)
R = R + DEL(I,J)
CONTINUE
C
C Area of sphere for source at center and detector at surface...
C
A = 4.0 * PI * R ** 2
C
C Multiply voltage signal by sphere area and divide by detector
C area to get total from source...
C
VO(I,1) = VO(I,1) * A
VO(I,1) = VO(I,1) / DETA
C
C VO is now per unit steradian...
C
C Termination resistance was 50 ohms...
C
VO(I,1) = VO(I,1) / 50.0
CONTINUE
TRES(I) = 0.0
RETURN
END

```



```
200 CONTINUE
188 CONTINUE
C
C Output initial spectrum, iteration/convergence parameters
C
C WRITE(3,200) SO , NP , ERMAX , KITMAX , NSPEC , T1 , T2
C
C SO is value for initial flat spectrum, if < 0 then
C two temperature DEXPonential is used instead.
C NP is
C ERMAX is average error allowed per detector for the
C completion of the convergence
C KITMAX is the maximum number of iterations allowed
C T1 and T2 are the temperatures to be used for the
C two temperature DEXPonential initial iteration
C
200 FORMAT( E16.8 , I5 , E16.8 , 2I5 , 2E16.8 )
C
C Output energy limits/number of groups/etc...
C
C WRITE(3,220) NE , E1 , RATIO , AA , BB
220 FORMAT(I5,4E16.8)
C
C Output initial detector signals and times...
C
C NTIMES = 1
DO 350 J = 1 , NTIMES
WRITE(3,300) ( VO(I,J) , I = 1 , NDET ) , TRES(J)
300 FORMAT(9E16.4)
350 CONTINUE
CLOSE(UNIT=3)
RETURN
END
```

APPENDIX E

APPENDIX E

Sample Input for Program PIN

This is a listing of sample input for program PIN. This input to PIN generated the sample input for program DCON in Appendix B. The explanations listed to the right of the input data have no effect upon the program. They should be included though, because they will aid the user in modifying the input.

SHOT D6-4
 NUMBER OF DETECTORS
 Serial number of detector 1
 Voltage signal from detector 1
 DETECTOR 1 HAS 3 FILTERS
 FIRST FILTER IS Fe
 Fe is \varnothing .9525 cm (3/8")
 SECOND FILTER IS Air
 Air is 365.552 cm = 140.375"
 THIRD FILTER IS Al
 Al is \varnothing .635 cm = 1/4"
 Serial number of detector 2
 Voltage signal from detector 2
 DETECTOR 2 HAS 3 FILTERS
 FIRST FILTER IS Fe
 Fe is \varnothing .9525 cm (3/8")
 SECOND FILTER IS Air
 Air is 356.87 cm = 140.5"
 THIRD FILTER IS Cu
 Cu is \varnothing .3175 (1/8")
 Serial number of detector 3
 Voltage signal from detector 3
 DETECTOR 3 HAS 3 FILTERS
 FIRST FILTER IS Fe
 Fe is \varnothing .9525 cm (3/8")
 SECOND FILTER IS Air
 Air is 358.14 cm (141")
 THIRD FILTER IS Pb
 Pb is \varnothing .15875 cm (1/16")
 Serial number of detector 4
 Voltage signal from detector 4
 DETECTOR 4 HAS 4 FILTERS
 FIRST FILTER IS Fe
 Fe is \varnothing .9525 cm (3/8")
 SECOND FILTER IS Air
 Air is 358.775 cm (141.25")
 THIRD FILTER IS Cu
 Cu is \varnothing .3175 (1/8")
 FOURTH FILTER IS Al
 Al is \varnothing .635 cm = 1/4"
 Serial number of detector 5
 Voltage signal from detector 5
 DETECTOR 5 HAS 3 FILTERS
 FIRST FILTER IS Fe
 Fe is \varnothing .9525 cm (3/8")
 SECOND FILTER IS Air
 Air is 359.7275 cm (141.625")
 THIRD FILTER IS Cu
 Cu is \varnothing .3175 (1/8")
 Flat Spectrum
 Value is 1.0
 Smoothing Chosen (because Pb is a filter)
 ERMAX
 HITMAX
 New Spectrum
 100 Energy groups
 LI
 RATIO

Bibliography

1. Belikov A. G. et al. "Creation of Fast Plasmoids with a Coaxial Source", Plasma Physics and Controlled Thermonuclear Fusion, (212-218), Proceedings of the Fourth Conference on Plasma Physics and Controlled Thermonuclear Fusion, Kharkov, May 1963. Edited by K. D. Sinel'nikov. Jerusalem: Israel Program for Scientific Translations, 1966.
2. Chen, Francis F. Introduction to Plasma Physics. Plenum Press, New York, 1974.
3. Degnan, J. H. et al. "Soft and Ultrasoft X-Ray Measurements of Air Force Weapons Laboratory SHIVA Imploding Liner," AIP Conference Proceedings No. 75; (264-269) Low Energy X-Ray Diagnostics-1981 (Monterey), edited by D. T. Atwood and B. L. Henke. New York: American Institute of Physics, 1981.
4. Eisberg, Robert and Robert Resnick. Quantum Physics of Atoms, Molecules, Solids, Nuclei, and Particles. John Wiley & Sons, New York, 1974.
5. S. Glasstone and R. H. Loveburg. Controlled Thermonuclear Reactions. New York: Van Nostrand, 1960.
6. Hubbell, J. H. Photon Cross Sections, Attenuation Coefficients, and Energy Absorption From 10 keV to 100 Gev. NSRDS-NBS 29. Center for Radiation Research National Bureau of Standards, Washington D.C. August 1969.
7. Hubbell, J. H. "Photon Mass Attenuation and Mass-Energy Absorption Coefficients for H, C, N, O, Ar, and Seven Mixtures from 0.1 keV to 20 MeV, Radiation Research, 70:58-81 (1977).
8. Johnson, Lee W. and R. Dean Riess. Numerical Analysis. Addison-Wesley, Reading, Massachusetts, 1982.
9. Kirkpatrick, Paul. "On the Theory and Use of Ross Filters," The Review of Scientific Instruments, 10: 186-191 (June 1939).
10. Kirkpatrick, Paul. "Theory and Use of Ross Filters. II" The Review of Scientific Instruments, 10: 223-229 (June 1939).
11. Knoll, Glenn F. Radiation Detection and Measurement. John Wiley & Sons, New York, 1979.

12. Len, Leck Keah. "The Snowplow and Deflagration Modes of Operation in Coaxial Plasma Guns", Phd thesis, Department of Chemical and Nuclear Engineering, University of New Mexico, August 1983.
13. Marshall, John. "Performance of a Hydromagnetic Plasma Gun," The Physics Of Fluids, 3: 134-135 (January-February 1960).
14. Ross, P. A. "Polarization of X-Rays," Physical Review, 28: 425 (August 1926).
15. Ross, P. A. "A New Method of Spectroscopy for Faint X-Radiations: Journal of the Optical Society of America and Review of Scientific Instruments 6: 433-437 (June 1928).
16. Silberstein, L. "Spectral Composition of an X-Ray Radiation determined from its Filtration Curve", Philosophical Magazine, 15 375-394 (February 1933).
17. Tominaga, Shoji. "The Estimation of X-Ray Spectral Distributions from Attenuation Data by means of Iterative Computation," Nuclear Instruments and Methods, 192: 415-421 (February 1982).
18. Turchi, Peter J. and William L. Baker. "Generation of High-Energy Plasmas by Electromagnetic Implosion," Journal of Applied Physics, 44: 4936-4945 (November 1973).
19. Twidell, J. W. "The Determination of X-Ray Spectra using Attenuation Measurements and a Computer Program," Physics in Medicine and Biology, 15: 529-539 (July 1970).

Vita

Captain Charles William Beason was born on 18 September 1955 in Dover, Delaware. He graduated from Kecoughtan High School in Hampton, Virginia in 1973 and attended Louisiana Tech University from which he received the degree of Bachelor of Science with a double major in Physics and Mathematics. Upon graduation he received a commission in the USAF through the ROTC program. He attended graduate classes at Louisiana Tech until entering active duty in October 1978. He served as a Computational Physics Research Officer at the Advanced Weapons Concepts Branch at the Air Force Weapons Laboratory until entering the Air Force Institute of Technology in September 1982.

Permanent address: P. O. Box 2015

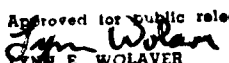
Alexandria, La. 71301

UNCLASSIFIED

SECURITY CLASSIFICATION OF THIS PAGE

AD-A172 756

REPORT DOCUMENTATION PAGE

1a. REPORT SECURITY CLASSIFICATION UNCLASSIFIED		1b. RESTRICTIVE MARKINGS										
2a. SECURITY CLASSIFICATION AUTHORITY		3. DISTRIBUTION/AVAILABILITY OF REPORT Approved for public release; Distribution unlimited										
2b. DECLASSIFICATION/DOWNGRADING SCHEDULE												
4. PERFORMING ORGANIZATION REPORT NUMBER(S) AFIT/GNE/PH/844-1		5. MONITORING ORGANIZATION REPORT NUMBER(S)										
6a. NAME OF PERFORMING ORGANIZATION School of Engineering Air Force Institute of Technology	6b. OFFICE SYMBOL (If applicable) AFIT/EN	7a. NAME OF MONITORING ORGANIZATION										
6c. ADDRESS (City, State and ZIP Code) Wright-Patterson AFB, OH 45433		7b. ADDRESS (City, State and ZIP Code)										
8a. NAME OF FUNDING/SPONSORING ORGANIZATION AFWL/INTYP	8b. OFFICE SYMBOL (If applicable) AFWL/INTYP	9. PROCUREMENT INSTRUMENT IDENTIFICATION NUMBER										
8c. ADDRESS (City, State and ZIP Code) Kirtland AFB MI 87117		10. SOURCE OF FUNDING NOS.										
		PROGRAM ELEMENT NO.	PROJECT NO.									
11. TITLE (Include Security Classification) See Box 19		TASK NO.	WORK UNIT NO.									
12. PERSONAL AUTHOR(S) Charles W. Beason, B.S., Capt, USAF												
13a. TYPE OF REPORT Thesis	13b. TIME COVERED FROM _____ TO _____	14. DATE OF REPORT (Yr., Mo., Day) 1984 March	15. PAGE COUNT 127									
16. SUPPLEMENTARY NOTATION												
17. COSATI CODES <table border="1"><tr><th>FIELD</th><th>GROUP</th><th>SUB. GR.</th></tr><tr><td>20</td><td>09</td><td></td></tr><tr><td></td><td></td><td></td></tr></table>		FIELD	GROUP	SUB. GR.	20	09					18. SUBJECT TERMS (Continue on reverse if necessary and identify by block number) Plasma(Physics); Plasma Devices; Plasma Diagnostics; X Ray Spectroscopy	
FIELD	GROUP	SUB. GR.										
20	09											
19. ABSTRACT (Continue on reverse if necessary and identify by block number) TITLE: A METHOD FOR DETERMINING THE HIGH ENERGY PHOTON SPECTRUM OF A PULSED PLASMA SOURCE												
Thesis Chairman: John F. Prince, Major, USAF		<p>Approved for public release: 1AW AFR 180-V  LYNN E. WOLAYER Dean for Research and Professional Development Air Force Institute of Technology (AFIT) Wright-Patterson AFB OH 45433</p>										
20. DISTRIBUTION/AVAILABILITY OF ABSTRACT UNCLASSIFIED/UNLIMITED <input checked="" type="checkbox"/> SAME AS RPT. <input type="checkbox"/> DTIC USERS <input type="checkbox"/>		21. ABSTRACT SECURITY CLASSIFICATION UNCLASSIFIED										
22a. NAME OF RESPONSIBLE INDIVIDUAL John F. Prince, Major, USAF		22b. TELEPHONE NUMBER (Include Area Code) 513-255-4498	22c. OFFICE SYMBOL AFIT/EP									

UNCLASSIFIED

SECURITY CLASSIFICATION OF THIS PAGE

> This investigation examined the feasibility of using an array of plastic scintillator photomultiplier tube radiation detectors to determine the high energy ($h\nu$ greater than 30keV) photon spectrum of SHIVA STAR. A method of determining the spectrum is outlined in which the detectors are filtered with different materials, and the spectrum is deconvoluted by an iterative technique on a computer. Data from SHIVA STAR was not available, so measurements of the γ radiation output of a plasma gun were analyzed.

UNCLASSIFIED

SECURITY CLASSIFICATION OF THIS PAGE

E A V D

W S 6

D T I C